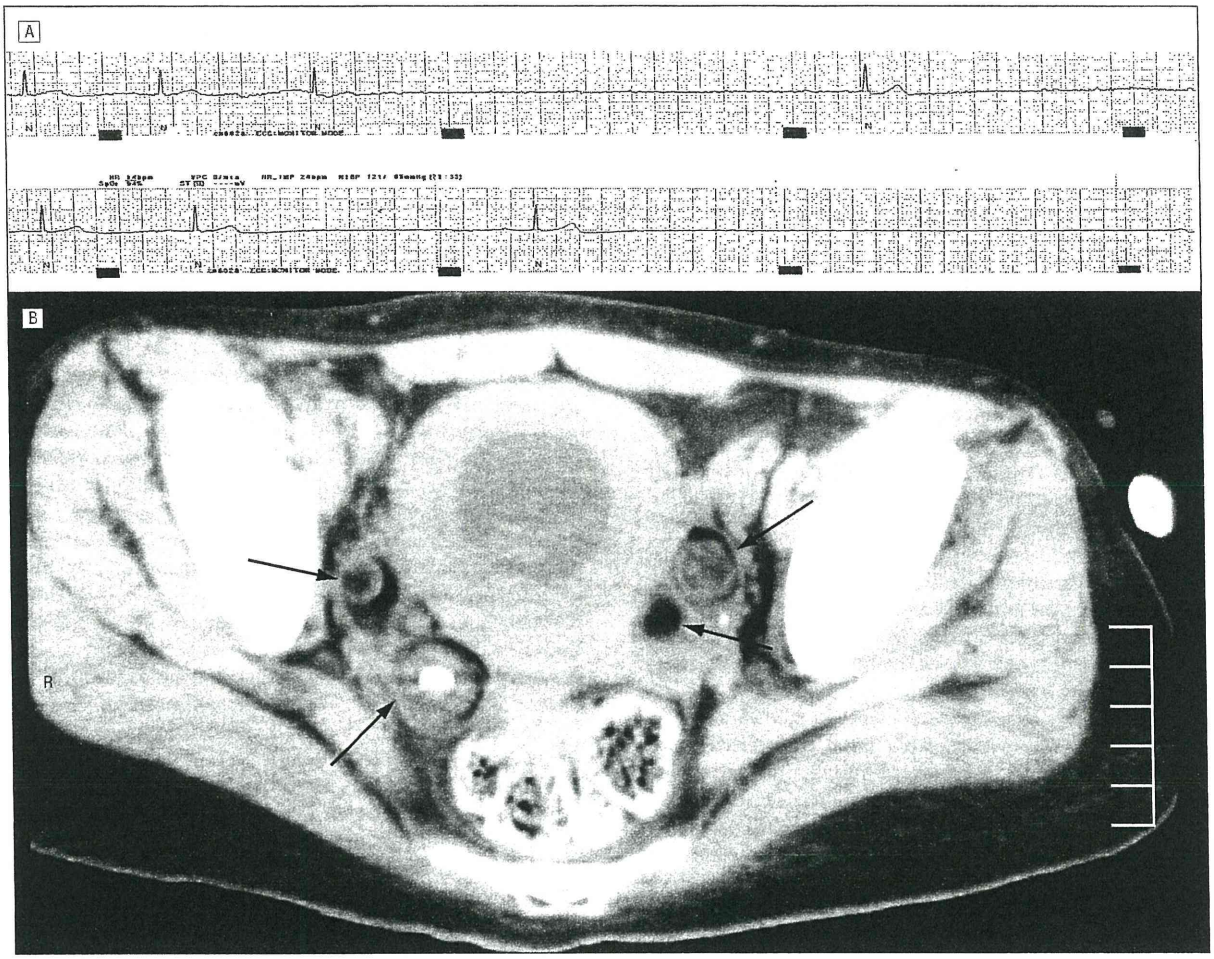

Figure. Cardiac pauses and bilateral teratomas in patient 2. A, Cardiac pauses up to 5 seconds were noted on day 3 of hospital admission. B, A pelvic computed tomographic scan revealed bilateral recurrent teratomas (arrows).

ing nervousness, irritability, and anxiety. She stopped walking and communicating but would say the same word repetitively and was transferred to a psychiatric facility. Her bizarre behavior continued; for example, she was frequently hitting the walls, taking cold baths, and accusing the physicians of "being murderers." She had fluctuating periods of decreased level of consciousness and agitation. She had a partial tonic seizure involving the left arm without EEG correlate; this showed generalized high-amplitude slow activity (2 Hz). Because of progressive deterioration and the presumptive diagnosis of viral encephalitis, she was transferred 1 week later to a neurology unit. On physical examination, her temperature was 37.1°C, and she had no neck stiffness. She developed hyperhidrosis and repetitive semirhythmic oral movements, like automatisms. Brain computed tomography and MRI were normal. The CSF showed lymphocytic pleocytosis (white blood cell count, 11/μL) with normal protein and glucose concentrations. Results of extensive viral studies and autoimmune and paraneoplastic markers were negative. Anti-NMDAR antibodies were identified in her serum and CSF. A second EEG showed no changes compared with the previous study. Magnetic resonance imaging of the abdomen and pelvis and abdominal ultrasonography were normal.

From day 19, the patient was treated with intravenous methylprednisolone (500 mg/d for 5 days) without clinical improvement, and a similar course of methylprednisolone treatment was started on day 35. After this second treatment, the orofacial dyskinesias subsided, but she continued with a decreased level of consciousness. On day 54, she had a generalized tonic-clonic seizure and treatment with phenobarbital was started. One month later, her level of consciousness started to progressively improve. Throughout the hospitalization, she did not develop hypoventilation. The fetus was monitored regularly by Doppler ultrasonography, showing normal heart tones. At 37 weeks of pregnancy, she spontaneously delivered a healthy 2892-g baby with Apgar scores of 8 at 1 minute and 9 at 5 minutes. Her Mini-Mental State Examination score was 24 of 30, and she was discharged 3 weeks later. At the last follow-up, she was fully functional and had returned to work. The child remains healthy with no obvious adverse effects.

DETECTION OF NMDAR ANTIBODIES

All 3 patients had higher NMDAR antibody titers in CSF than serum (Table). No antibodies were identified in the amniotic fluid, umbilical cord blood, serum, or CSF from the baby of patient 1. The baby of the other patient was not examined for antibodies.

COMMENT

To our knowledge, these are the first reported patients with anti-NMDAR encephalitis diagnosed during pregnancy. The 3 patients had substantial neurological recoveries, although in 1 case the pregnancy was terminated because of the severity of neurological symptoms, presence of recurrent bilateral teratomas, and early stage of pregnancy. The newborns of the other 2 patients were healthy and their physical and cognitive milestones are being closely followed up. Concern for the fetus and newborns is warranted in this disorder as studies indicate that NR1 antibodies from patients decrease NMDAR clusters in vitro and in animal models.[1,3] Moreover, the antibodies are IgG1 and IgG3, which are the subtypes involved in autoimmune newborn illnesses, such as congenital lupus.[4]

The good outcome of the 2 neonates of our study is likely due to several factors, including the variable effects of autoimmune disorders on the fetus. For example, despite experimental models showing that Ro/SSA antibodies cause congenital heart block, only 2% to 5% of neonates from patients with these antibodies have congenital heart block.[5] Two additional factors relate to the levels of serum maternal antibodies and the timing of transplacental transfer of IgG. IgG1 and IgG3 cross the placenta by binding to an Fc neonatal receptor present in syncytiotrophoblasts.[6] This mechanism of placental transfer develops around weeks 14 to 16, resulting initially in very low levels of fetal blood IgG that gradually increase until the time of delivery.[4] Additionally, the fetal blood-brain barrier becomes functional by the end of the second trimester. Our patients developed symptoms between 8 and 17 weeks of pregnancy when the IgG placental transfer is absent or limited, and assuming the immune response was triggered systemically, the levels of serum NMDAR antibodies decreased rapidly. In fact, 2 patients had negative serum but positive CSF antibody titers (both tested at initial dilution 1:10) by the time they were diagnosed with anti-NMDAR encephalitis, explaining the absence of NMDAR antibodies in the baby who was tested.

With a sharp increase in the number of cases with anti-NMDAR encephalitis, more patients will be identified during pregnancy. This study suggests that these patients and the newborns can do well. The concern should be the search (and removal) of a teratoma along with supportive care of the mother and fetus. Treatment with corticosteroids, intravenous immunoglobulin, and plasmapheresis was well tolerated but the effects could not be assessed because of the close temporal association with tumor removal in 2 patients. The third patient only received corticosteroids, with questionable improvement of the dyskinesias. The recovery seemed to accelerate after giving birth; this and the predominance of the disorder in young women bring into consideration a possible role of hormonal factors that needs further study.

Accepted for Publication: February 8, 2010.
Correspondence: Josep Dalmau, MD, PhD, Department of Neurology, 3 W Gates, University of Pennsylvania, 3400 Spruce St, Philadelphia, PA 19104 (josep.dalmau@uphs.upenn.edu).
Author Contributions: Drs Kumar, Dechant, and Saito and Mr Jain contributed equally to this work. *Study concept and design:* Dechant and Dalmau. *Acquisition of data:* Kumar, Jain, Dechant, Saito, Rafael, Dysart, Ito, Araki, Abe, and Dalmau. *Analysis and interpretation of data:* Kumar, Jain, Aizawa, Katayama, Balice-Gordon, and Dalmau. *Drafting of the manuscript:* Kumar, Dechant, Saito, Aizawa, and Dalmau. *Critical revision of the manuscript for important intellectual content:* Jain, Dechant, Rafael, Dysart, Katayama, Ito, Araki, Abe, Balice-Gordon, and Dalmau. *Obtained funding:* Balice-Gordon and Dalmau. *Administrative, technical, and material support:* Dysart, Katayama, Ito, Araki, Abe, and Dalmau. *Study supervision:* Kumar, Balice-Gordon, and Dalmau.
Financial Disclosure: Dr Dalmau has received royalties from a patent related to an Ma2 autoantibody test, filed patent applications for NMDA and γ-aminobutyric acid B receptor autoantibody tests, and received funding from Euroimmun for projects unrelated to the current study.
Funding/Support: This study was supported in part by National Institutes of Health grant 1RC1NS068204-01 (Drs Balice-Gordon and Dalmau).
Additional Contributions: Yoko Aburakawa, MD, PhD, and Naoyuki Hasebe, MD, PhD, Asahikawa Medical College, Asahikawa, Hokkaido, Japan, and Ryo Tomioka, MD, Saitama Medical University, Moroyama, Saitama, Japan, provided clinical information.

REFERENCES

1. Dalmau J, Gleichman AJ, Hughes EG, et al. Anti-NMDA-receptor encephalitis: case series and analysis of the effects of antibodies. *Lancet Neurol.* 2008;7(12):1091-1098.
2. Tüzün E, Zhou L, Baehring JM, Bannykh S, Rosenfeld MR, Dalmau J. Evidence for antibody-mediated pathogenesis in anti-NMDAR encephalitis associated with ovarian teratoma [published online August 14, 2009]. *Acta Neuropathol.* 2009. doi:10.1007/s00401-009-0582-4.
3. Hughes EG, Peng X, Gleichman AJ, et al. Cellular and synaptic mechanisms underlying anti-NMDA receptor encephalitis. *Ann Neurol.* 2009;66(suppl 13):S63-S64.
4. Hoftman AC, Hernandez MI, Lee KW, Stiehm ER. Newborn illnesses caused by transplacental antibodies. *Adv Pediatr.* 2008;55:271-304.
5. Brucato A, Doria A, Frassi M, et al. Pregnancy outcome in 100 women with autoimmune diseases and anti-Ro/SSA antibodies: a prospective controlled study. *Lupus.* 2002;11(11):716-721.
6. Roopenian DC, Akilesh S. FcRn: the neonatal Fc receptor comes of age. *Nat Rev Immunol.* 2007;7(9):715-725.

Neuron

Retinoid X Receptor Gamma Control of Affective Behaviors Involves Dopaminergic Signaling in Mice

Agnieszka Krzyżosiak,[1,2,3,6] Monika Szyszka-Niagolov,[1,2,6] Marta Wietrzych,[1,2] Serge Gobaille,[4] Shin-ichi Muramatsu,[5] and Wojciech Krężel[1,2,*]

[1]IGBMC (Institut de Génétique et de Biologie Moléculaire et Cellulaire), BP 10142, Inserm, U 596, CNRS, UMR 7104 Illkirch F-67400, France
[2]Université de Strasbourg, Strasbourg F-67000, France
[3]Wrocław University of Technology, Faculty of Chemistry, Division of Biochemistry, Wybrzeże Wyspiańskiego 27, 50-370 Wrocław, Poland
[4]IFR37 de Neurosciences, Faculté de Médecine, 11 rue Humann, 67085 Strasbourg, France
[5]Division of Neurology, Department of Medicine, Jichi Medical University, 3311-1 Yakushiji, Shimotsuke, Tochigi 329-0498, Japan
[6]These authors contributed equally to this work
*Correspondence: krezel@igbmc.u-strasbg.fr
DOI 10.1016/j.neuron.2010.05.004

SUMMARY

Abnormal signaling by retinoids or n-3 polyunsaturated fatty acids has been implicated in clinical depression. The converging point in activities of these two classes of molecules is transcriptional activation of retinoid X receptors (Rxr). We show here that ablation of *Rxrγ* in mice leads to depressive-like behaviors including increased despair and anhedonia, which were accompanied by reduced expression of dopamine D2 receptor in the shell of nucleus accumbens (NAc) and altered serotonin signaling. While abnormal serotonin signaling is not sufficient to generate the depressive behaviors, increasing D2r expression by chronic fluoxetine (Prozac) treatment or adenoassociated virus type2 (AAV2) mediated expression of Rxrγ or D2r in the NAc of *Rxrγ*$^{-/-}$ mice normalizes depressive-like behaviors in *Rxrγ*$^{-/-}$ animals. Conversely, NAc infusion of raclopride, a D2r antagonist prevents AAV2-*Rxrγ*-mediated rescue of despair behaviors in *Rxrγ*$^{-/-}$ mice. Combined, our data argue that control of NAc D2r expression is critical for Rxrγ-mediated modulation of affective behaviors.

INTRODUCTION

Dopaminergic signaling and in particular its mesolimbic pathway plays an important, reinforcing role in regulation of motivated behaviors. Abnormally low dopaminergic signaling has been suggested to be involved in clinical depression (Millan, 2006; Nestler and Carlezon, 2006). Classical antidepressant treatments increase dopaminergic tone and its signaling via different dopamine receptor subtypes, which suggests a direct implication of dopamine in the efficiency of such treatments (Renard et al., 2001; Valentini et al., 2004; Willner et al., 2005). The dopaminergic reuptake inhibitor, Bupropion, has been found effective as an antidepressant treatment (Foley et al., 2006), although its actions also implicate noradrenergic transmission. Furthermore, some of the dopaminergic receptor ligands, such as bromocriptine and pergolide or pramipexole, are effective in the treatment of depression either as a monotherapy or as adjuvants (Corrigan et al., 2000; Mattes, 1997; Theohar et al., 1982). Although the dopamine receptor specificity of these agents is variable, all of them act as agonists of dopamine D2 receptor (D2r), which suggests that this receptor plays a particular role in the regulation of affective behaviors. This possibility is further supported by preclinical studies in rodent models used for research on depression. Thus, chronic mild stress leads to a reduction of D2r expression in the nucleus accumbens (Willner, 1997), and activation of D2 receptors has an anti-depressant action in animal models of despair (Brocco et al., 2006; Siuciak and Fujiwara, 2004). Moreover, chronic antidepressant treatments including selective serotonin reuptake inhibitors (SSRIs), which primarily modulate serotonergic transmission, can also increase D2r expression in humans and rodents (Ainsworth et al., 1998; Dziedzicka-Wasylewska et al., 1997; Larisch et al., 1997). In line with such findings, an inhibition of D2r in human and animal models prevents antidepressant activities of fluoxetine (Prozac) and/or other antidepressants (Willner et al., 2005, and references therein).

The expression of D2r is modulated at the transcriptional level by retinoic acid (RA), an active form of vitamin A (Krezel et al., 1998; Samad et al., 1997). Such control implicates activities of retinoic acid receptors (Rarα, Rarβ, Rarγ) and retinoid X receptors (Rxrα, Rxrβ, Rxrγ), which in the form of heterodimers act as transcription factors and mediate RA signaling in vivo (Kastner et al., 1997). Rarβ and Rxrγ are the predominant retinoid receptors expressed in the striatum, including the nucleus accumbens (Krezel et al., 1999; Zetterström et al., 1999). Concomitant ablation of these receptors in *Rarβ/Rxrγ* double-knockout mice leads to strong reduction of D2r expression in the dorsal and ventral striatum and marked locomotor deficits (Krezel et al., 1998). The involvement of murine retinoid receptors in the control of dopaminergic signaling in the striatum might suggest a potential role of the retinoid pathway in modulation of affective behaviors. Such modulation is further suggested by clinical data on depression associated with altered retinoid signaling in *acne vulgaris* patients treated with isotretinoin (Bremner and McCaffery,

2008). Rxr's were also proposed to mediate genomic actions of n-3 polyunsaturated fatty acids (n-3 PUFAs) (de Urquiza et al., 2000; Lengqvist et al., 2004). Such functions of Rxrs could be directly relevant for the pathology of affective disorders, as decreased n-3 PUFA signaling has been suggested to be associated with depression and use of n-3 PUFAs such as docosahexaenoic acid or eicosapentaenoic acid were reported beneficial in clinical conditions (Logan, 2004; Peet and Stokes, 2005) and in animal models used in research on depression (Carlezon et al., 2005; Naliwaiko et al., 2004). We have combined pharmacological and genetic approaches to address the role of retinoid receptors in control of affective behaviors and implication of dopaminergic signaling in such control.

RESULTS

Increased Despair Behaviors in *Rxrγ* Null Mice Can Be Normalized by Antidepressant Treatment

To address the contribution of retinoid receptors in control of despair behaviors we have studied the effects of the loss of function of Rarβ and/or Rxrγ in mice on performance in the forced swim test. Concomitant ablation of *Rarβ* and *Rxrγ* in $Rar\beta^{-/-}$ $Rxr\gamma^{-/-}$ double null mutant mice led to a marked increase of the immobility time, which attained 129 ± 4.3 s and was significantly longer ($p < 0.001$) than in wild-type (WT) control mice, which remained immobile for 71 ± 6.2 s (Figure 1A). The increased immobility in the double-mutant mice was principally due to the loss of function of Rxrγ, since single $Rxr\gamma^{-/-}$ mutants displayed similar high immobility time of 117 ± 4 s, whereas inactivation of Rarβ did not affect immobility time in this task (64.9 ± 6.8 s; $p > 0.05$). An abnormal locomotor behavior is unlikely to account for the increased immobility time of $Rxr\gamma^{-/-}$ mice in the forced swim test, since $Rxr\gamma^{-/-}$ mice did not differ from their WT littermates with respect to spontaneous locomotion in actimetric cages, novelty-induced locomotion in the open field test, or locomotor coordination in the rotarod task (Krezel et al., 1998; see Figure S1 available online).

Since despair behaviors belong to the core symptoms of depression, we have explored whether antidepressant treatment could improve the performance of $Rxr\gamma^{-/-}$ mice. In agreement with previous reports of SSRI activities in C57BL6J and 129SV mouse strains (Dulawa et al., 2004), a 21 day chronic treatment with fluoxetine at the dose of 20 mg/kg/24hr did not affect performance of WT mice in the forced swim test, but such treatment reversed the despair behavior in $Rxr\gamma^{-/-}$ mice (Figure 1B), as illustrated by a significant *genotype* × *fluoxetine* treatment interaction ($F[1,35] = 23.2$, $p < 0.001$). Thus, high immobility of vehicle treated $Rxr\gamma^{-/-}$ mice was reduced in fluoxetine treated $Rxr\gamma^{-/-}$ animals, which behaved comparably to vehicle treated WT mice (Figure 1B).

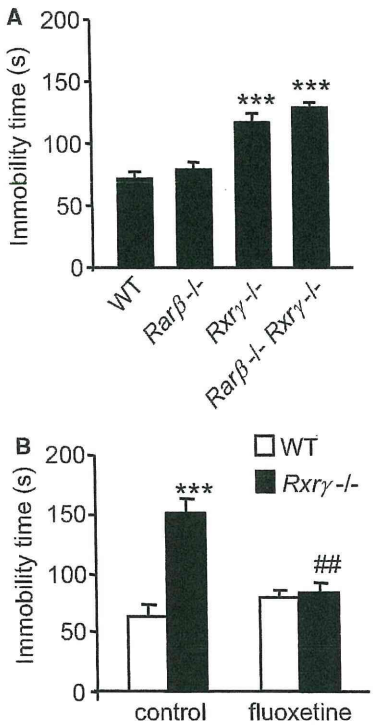

Figure 1. Increased Despair Behavior in *Rxrγ*$^{-/-}$ Null Mutant Mice Is Reversible by Chronic Antidepressant Treatment

The time of immobility in the forced swim test was measured in naive $n_{WT} = 6$ and $n_{Rar\beta-/-} = 8$, $n_{Rxr\gamma-/-} = 8$ single- and $n_{Rar\beta-/-Rxr\gamma-/-} = 8$ double-mutant littermates (A). Chronic, 21-day long treatment with fluoxetine (20 mg/kg/24 hr) reduced the immobility time in $n_{Rxr\gamma-/-} = 10$ mice as compared to $n_{Rxr\gamma-/-} = 10$ mice fed with control diet but not in $n_{WT} = 8$ mice as compared to $n_{WT} = 11$ mice fed with control diet (B). Data are presented as mean values ± SEM. ***$p < 0.001$ with respect to nontreated (A) or vehicle-treated (B) WT mice; $^{\#\#}p < 0.01$ as compared with vehicle-treated $Rxr\gamma^{-/-}$ mice. See also Figure S1.

Inactivation of Rxrγ Leads to Anhedonia, Which Can Be Normalized by Antidepressant Treatment

To better evaluate the involvement of retinoid receptors in the control of affective behaviors, we investigated hedonic behaviors in the sucrose preference test in $Rar\beta^{-/-}$ and $Rxr\gamma^{-/-}$ single and compound mutant mice. During the active, night phase of the circadian cycle WT mice displayed clear preference for a 1% sucrose solution as compared to plain water, since sucrose represented 91.3% ± 2.7% of total liquid consumption. In compound $Rar\beta^{-/-}Rxr\gamma^{-/-}$ mutant mice, such a preference was absent as sucrose consumption reached 58.1% ± 10.6% of total liquid intake (Figure 2A), which was significantly less than preference in WT mice ($p < 0.05$) and not different from a chance level of 50% ($t = -0.1$, ns, one-group t test). Such anhedonic behavior was due to ablation of *Rxrγ*, since *Rxrγ* single null mutants displayed similar loss of sucrose preference and consumed 57.8% ± 10.8% of sucrose solution, whereas $Rar\beta^{-/-}$ mice consumed sucrose solution at 92% ± 2.1% and were indistinguishable from their WT controls. The total liquid intake during the sucrose preference test was not different between WT and mutant mice (4.6 ± 0.2 g for WT, 4.9 ± 0.3 for $Rar\beta^{-/-}$, 4.9 ± 0.2 for $Rxr\gamma^{-/-}$ and 5.2 ± 0.3 for $Rar\beta^{-/-}Rxr\gamma^{-/-}$ mutants). The absence of sucrose preference in $Rar\beta^{-/-}$ $Rxr\gamma^{-/-}$ and $Rxr\gamma^{-/-}$ mice is unlikely to result from gustative deficits since all groups preferred water to 1% sucrose on the first presentation of sucrose drink. Thus, during 3 hr of the first

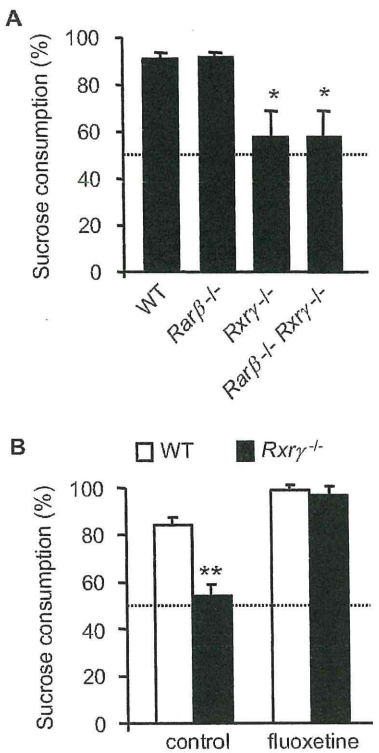

Figure 2. Loss of Sucrose Preference in *Rxrγ*$^{-/-}$ Mice Is Reversible by Chronic Antidepressant Treatment

Sucrose preference was measured as percent of sucrose solution consumption with respect to total amount of liquid consumed during the night phase in n_{WT} = 11 and $n_{Rarβ-/-}$ = 11, $n_{Rxγ-/-}$ = 7, and $n_{Rarβ-/-Rxrγ-/-}$ = 7 null mutant mice (A). Chronic, 19-day long treatment with fluoxetine (20 mg/kg/24 hr) normalized sucrose preference in $n_{Rxrγ-/-}$ = 18 mice as compared to $n_{RXRγ-/-}$ = 22 mice fed with control diet but not in n_{WT} = 13 mice as compared to n_{WT} = 15 mice fed with control diet (B). Data are presented as mean values ± SEM. *p < 0.05 significantly different from WT group; **p < 0.01 different from vehicle treated WT mice.

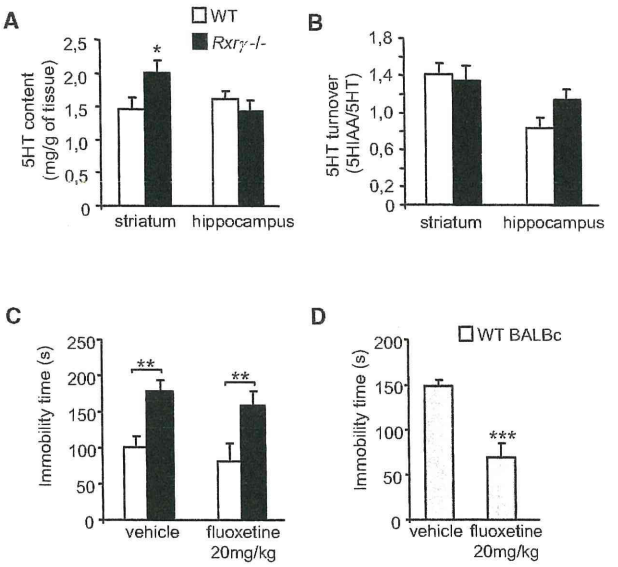

Figure 3. Abnormal Serotonergic Signaling Is Not Sufficient to Generate Despair Behavior in *Rxrγ*$^{-/-}$ Mice

Total tissue levels of 5HT were standardized by tissue weight and compared for the hippocampus and striatum in n_{WT} = 6 and $n_{Rxrγ-/-}$ = 6 mice (A). For the same animals and structures the serotonin turnover was calculated as ratio of standardized measures of 5HIAA and 5HT (B). Acute treatment with fluoxetine (20 mg/kg) did not alter immobility time in the forced swim test neither in $n_{Rxrγ-/-}$ = 8 mice as compared to $n_{Rxrγ-/-}$ = 8 vehicle-treated mice nor in n_{WT} = 7 mice as compared to n_{WT} = 9 vehicle-treated mice (C), whereas the same dose significantly reduced immobility time in control strain of n_{BALBc} = 6 mice as compared to n_{BALBc} = 6 vehicle-treated mice (D). Data are presented as mean values ± SEM. *p < 0.05 or **p < 0.01 for selected comparisons and ***p < 0.001 in comparison with vehicle treated BALBc mice.

testing session, in sucrose-naive WT mice sucrose solution constituted 43% ± 2.5% of total liquid consumption, as compared to 44% ± 2.1% for *Rarβ*$^{-/-}$, 37% ± 5% for *Rxrγ*$^{-/-}$, and 32.4% ± 7.3% for *Rarβ*$^{-/-}$*Rxrγ*$^{-/-}$ mice, which for all groups was significantly less than the chance level of 50% (t > 3.5 for any of the comparisons, p < 0.05, one-group t test). Such avoidance of sucrose solution by sucrose-naive mice results from a natural tendency for reserved consumption of novel food/drink and provides evidence for recognition of 1% sucrose taste. A chronic, 19 day antidepressant treatment with 20 mg/kg/24hr of fluoxetine, reversed the sucrose preference deficits in *Rxrγ*$^{-/-}$ mice (Figure 2B), which is reflected by significant *genotype* × *treatment* interaction (F[1,64] = 7.9, p < 0.01). Thus, fluoxetine-treated *Rxrγ*$^{-/-}$ mice preferred sucrose solution to water similarly to WT control mice, and the percentage of sucrose solution consumed by fluoxetine-treated *Rxrγ*$^{-/-}$ mice was significantly higher than in vehicle-treated mutant animals (p < 0.001).

Abnormal Serotonergic Signaling Is Not Sufficient to Generate Depressive Behaviors in *Rxrγ*$^{-/-}$ Mice

Efficiency of fluoxetine to reverse affective abnormalities could suggest that altered serotonergic signaling is at the origin of depressive-like behaviors in *Rxrγ*$^{-/-}$ mice. To address this issue, we carried out global evaluation of serotonergic signaling focusing on hippocampus and striatum (including NAc), the two regions differentially innervated by dorsal and median raphe 5HT inputs suggested to play a role in control of affect (Lechin et al., 2006). HPLC measurements of 5HT and its metabolite 5HIAA in tissue homogenates revealed a significant increase of 5HT levels in the striatum of *Rxrγ*$^{-/-}$ mice (2.01 ± 0.18 ng/g for *Rxrγ*$^{-/-}$ and 1.46 ± 0.17 for WT mice; t = 2.2, p = 0.05), which was not accompanied by altered metabolism of serotonin (Figure 3A). Although there was no significant difference in 5HT levels in the hippocampus, *Rxrγ*$^{-/-}$ displayed strong tendency (t = 1.92, p = 0.08) for increased metabolism of 5HT in this region (Figure 3B). Such abnormalities in the distribution of 5HT did not correlate with abnormal expression of 5HT1a receptor, prominently involved in control of 5HT tone and proposed to play a role in control of affective behaviors and in actions of SSRI antidepressants (Blier et al., 1998; Blier and Ward, 2003). Indeed, the relative *5HT1a* mRNA levels (standardized with respect to

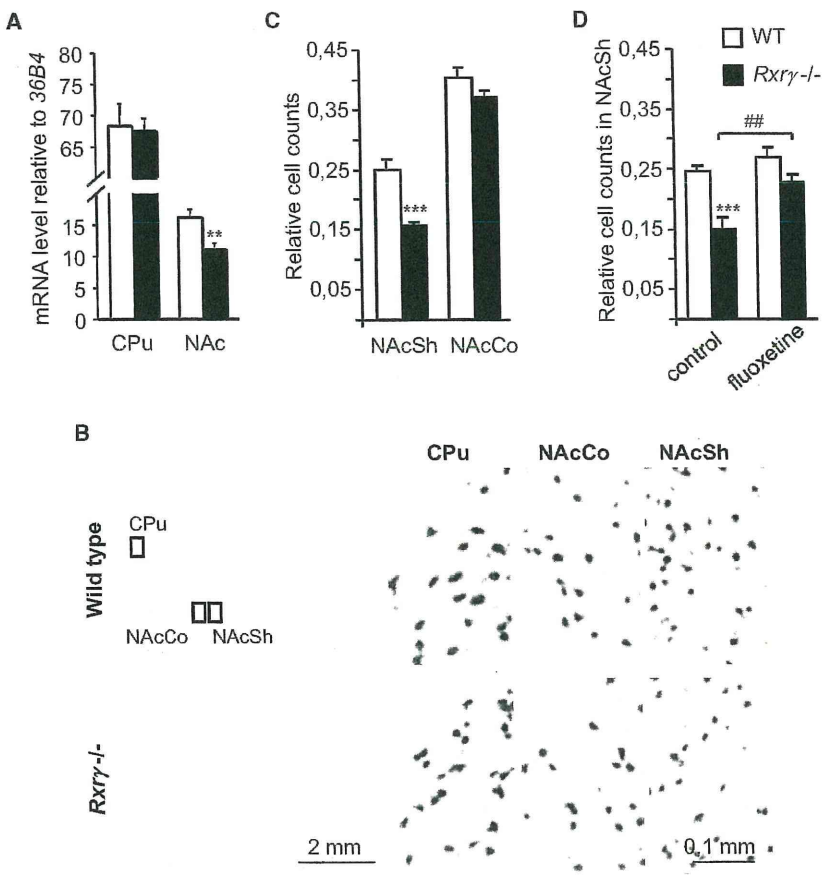

Figure 4. Decreased Expression of Dopamine D2r Receptor mRNA in the Nucleus Accumbens of *Rxrγ*$^{-/-}$ Mice Is Reversed by Chronic Fluoxetine Treatment

D2r mRNA levels were measured by quantitative real-time RT-PCR and are presented as relative to the expression of the housekeeping gene 36B4, $n_{WT} = 9$, $n_{Rxr\gamma-/-} = 10$ (A). In situ hybridization detection of D2r mRNA is shown in the whole striatum (left), and at high magnification in selected regions (boxed) of the caudate putamen (CPu), nucleus accumbens shell (NAcSh), and core (NAcCo) in WT and *Rxrγ*$^{-/-}$ mice (B). The numbers of D2r-positive cells in the shell and core of the NAc are presented as relative to D2r cell counts in the adjacent dorsal part of the CPu on the same section, for $n_{WT} = 6$ and $n_{Rxr\gamma-/-} = 6$ mice (C). The effects of 19 days of chronic fluoxetine treatment on the relative numbers of D2r positive cells in NAcSh in $n_{WT} = 3$ and $n_{Rxr\gamma-/-} = 5$ mice were compared with $n_{WT} = 4$ and $n_{Rxr\gamma-/-} = 4$ mice fed control diet (D). Data are presented as mean values ± SEM. $^{**}p < 0.01$; $^{***}p < 0.001$ different from corresponding WT group or ##, $p < 0.01$ for selected comparison. See also Figure S2.

expression of the house keeping gene *36B4*) were comparable between *Rxrγ*$^{-/-}$ and their WT controls in the NAc (2.2 ± 0.4 for *Rxrγ*$^{-/-}$ and 2.7 ± 0.3 for WT; t = −1, ns) and hippocampus (1.4 ± 0.2 for *Rxrγ*$^{-/-}$ and 1.9 ± 0.3 for WT mice; t = −1.5, ns).

To investigate functional relevance of abnormal serotonergic signaling for depressive-like behaviors in *Rxrγ*$^{-/-}$ mice we have tested whether acute fluoxetine treatment can reverse increased despair in the forced swim test. In contrast to chronic treatment, acute administration of fluoxetine at 20 mg/kg (IP, 30min prior to the forced swim test) did not alter increased immobility of *Rxrγ*$^{-/-}$ mice as there was no significant interaction for *genotype* × *fluoxetine* treatment (F[1,28] = 3E-4, ns) and the main effect of *genotype* (F[1,28] = 19.4, $p < 0.001$) remained significant despite of the treatment (Figure 3C). To control for the efficiency of acute fluoxetine treatment we used wild-type BALBcByJ (BALBc) mice, the strain susceptible to reveal antidepressant activities of fluoxetine (Lucki et al., 2001), and we found that 20 mg/kg of fluoxetine was sufficient to significantly reduce despair behaviors in this strain (Figure 3D). We concluded that inefficiency of acute fluoxetine treatment to modulate despair behaviors suggests that abnormal serotonergic signal is not sufficient to generate depressive behaviors and adaptive changes associated with chronic fluoxetine treatments might be at the origin of affective abnormalities in *Rxrγ*$^{-/-}$ mice.

Reduced Dopamine D2 Receptor Signaling in the Nucleus Accumbens of *Rxrγ*$^{-/-}$ Mice Is Reversible by Fluoxetine Treatment

The despair behavior and anhedonia and their reversal by chronic antidepressant treatment in *Rxrγ*$^{-/-}$ mice, indicates that null mutation of *Rxrγ* leads to deficits resembling some of the core symptoms of depression. We hypothesized that abnormal function of the nucleus accumbens (NAc), the key structure implicated in the control of motivated behaviors and one of the primary sites of Rxrγ expression (Krezel et al., 1999) might be at the origin of the behavioral abnormalities in *Rxrγ*$^{-/-}$ mice. As dopaminergic signaling in the NAc is critically involved in the modulation of motivated behaviors and in the mechanisms of antidepressant activities including fluoxetine, we examined the expression of dopaminergic D1 and D2 receptors in *Rxrγ*$^{-/-}$ mice. Using real-time quantitative RT-PCR, we found a significant 32% reduction of *D2r* expression in the NAc of *Rxrγ*$^{-/-}$ mice (t = −3.16, $p < 0.01$; Figure 4A). Interestingly, no such reduction (t = −0.22, ns) was observed in the dorsal caudate putamen (CPu). The inactivation of Rxrγ did not affect expression of D1r as *D1r* RNA levels were not significantly different between WT and *Rxrγ*$^{-/-}$ mice in the NAc (11.7 ± 1.0 versus 10.6 ± 1.0 units; t = −0.76, ns) and dorsal striatum (37.2 ± 2.2 versus 39.9 ± 0.8 units; t = 1.35, ns), as measured by RT-PCR and calculated relative to expression of a reference housekeeping gene (Figure S2).

In order to further investigate the regionalization and the origin of reduced levels of D2r mRNA in the NAc we carried out in situ hybridization (ISH) studies (Figure 4B). Comparisons of *Rxrγ*$^{-/-}$ mice and their WT controls revealed that the number of neurons

expressing D2r was significantly reduced in the shell of the NAc (152 ± 4 versus 206 ± 6; t = −8, p < 0.001) and the core of the NAc (294 ± 6 versus 338 ± 16; t = −2.44; p < 0.05), but not in the dorsal striatum (798 ± 17 versus 841 ± 34; t = −1.1, ns). To minimize cell counting errors related to differences in the signal intensity between different sections, which may account for more discrete changes, we took advantage of expression of D2r in the dorsal striatum (CPu), which was not affected by ablation of *Rxrγ*$^{-/-}$ and we used this region as our internal (intra-section) control to calculate relative changes in D2r cell numbers. To this end we divided cell counts in the NAcSh or NAcCo by those obtained for the adjacent region of CPu on the same section. We found a strong (36%) reduction in relative cell number only in the NAcSh (0.16 ± 0.01 for *Rxrγ*$^{-/-}$ as compared to 0.25 ± 0.02 for WT; t = −4.7, p = 0.001), but not in the NAcCo (0.37 ± 0.01 for *Rxrγ*$^{-/-}$ versus 0.40 ± 0.02 for WT; t = −1.5, ns), of *Rxrγ*$^{-/-}$ mice (Figure 4C). The difference in the magnitude of changes in D2r expression might be related to much weaker expression of Rxrγ in the NAcCo as compared to shell region (Krezel et al., 1999). Reduction of D2r in the NAcSh might be functionally relevant as chronic fluoxetine treatment, in addition to reversing depressive-like behaviors, increased also the relative number of D2r positive cells in the NAcSh of behaviorally naive *Rxrγ*$^{-/-}$ mutants (0.15 ± 0.02 for nontreated *Rxrγ*$^{-/-}$ versus 0.23 ± 0.01 for fluoxetine treated *Rxrγ*$^{-/-}$ mice; t = −3.4, p < 0.01), but not WT mice (0.24 ± 0.01 for nontreated WT versus 0.27 ± 0.02 for fluoxetine treated mice; t = −1.2, ns; Figure 4D).

A decrease of D2r-positive cell number in the NAcSh of *Rxrγ*$^{-/-}$ mice is most probably related to reduced transcription of D2r, rather than to the loss of a subpopulation of D2r expressing neurons. Supporting this hypothesis, the number of cells expressing mRNA coding for enkephaline, a neuropeptide found predominantly in D2r expressing neurons, was not significantly reduced (124.3 ± 2.8 enkephaline-positive cells in the NAc shell of *Rxrγ*$^{-/-}$ mice, as compared to 133.6 ± 3 cells in WT animals; t = −2.34, ns). Thus, the reduced number of D2r-expressing neurons could reflect a general decrease of D2r transcription in the NAc shell, with a reduction below the detection threshold level in neurons expressing low levels of D2r. Alternatively, it might be related to reduced transcriptional control of D2r restricted to a selected neuronal population. To address this issue, we quantified the intensity of D2r expression in the ISH experiments, using the ImageJ software (see Experimental Procedures). We found that the mean intensity of the D2r signal in the NAc shell was not different between WT and *Rxrγ*$^{-/-}$ mice when comparing absolute mean values (122.9 ± 2.2 for WT and 125.1 ± 2 for *Rxrγ*$^{-/-}$ mice; t = 0.7, ns) or when such measures were normalized with respect to the intensity of D2r expression in the dorsal striatum within the same brain section, where D2r expression was not affected by ablation of Rxrγ (1.05 ± 0.01 for WT and 1.08 ± 0.02 for *Rxrγ*$^{-/-}$ mice; t = 1, ns). These data suggest that Rxrγ might control expression of D2r in a selected subpopulation of D2r neurons.

Finally, to assess whether cell- and regional-specific reduction of *D2r* mRNA expression leads to abnormal D2r activities, we investigated neuronal activation in *Rxrγ*$^{-/-}$ mice in response to haloperidol, a D2 preferential antagonist. To this end, we studied the induction of c-*fos* protein expression, a molecular marker related to neuronal activity and plasticity. An acute treatment with haloperidol (1 mg/kg) increased the number of c-*fos* positive cells in various regions of the striatum, including the shell and core of the NAc and CPu in all tested mice (Figures 5A and 5B). However, in the shell of the NAc the magnitude of this increase was significantly lower in the in *Rxrγ*$^{-/-}$ than in WT mice as reflected by the significant interaction between *genotype* and *treatment* (F[1,14] = 5.6, p < 0.05) and PLSD Fischer post hoc analysis (p < 0.01). Such difference was not observed in the core of the NAc or in the dorsal CPu in the same sections (compare NAc-Sh with NAc-Co and CPu for WT-Hal and KO-Hal in Figure 5C). To study whether such a decrease reflects the action of haloperidol or is related to the stress inflicted during drug injection, we also evaluated the numbers of c-*fos* positive cells in saline-injected mice and found that these numbers were not significantly different between WT and *Rxrγ*$^{-/-}$ mice (compare WT-veh and KO-veh in Figure 5C). Thus, the haloperidol-specific induction of c-*fos* in the shell of the NAc, calculated as the ratio of c-*fos* positive cells in the haloperidol-treated mice with respect to saline-treated mice, was lower by 48% in *Rxrγ*$^{-/-}$ mice as compared to their WT controls (Figure 5D). To validate these findings functionally we tested the locomotor effects of low, non-cataleptic doses of haloperidol, which have been proposed to involve post-synaptic dopamine D2 receptors in the nucleus accumbens (Messier et al., 1992; Millan et al., 2004; Pijnenburg et al., 1976). All mice treated with haloperidol displayed reduction of locomotor activity in the novel environment of the open field, although such reduction was different depending on the genotype (significant *genotype* × *treatment* interaction, F[4,68] = 2.7; p < 0.05). Post hoc analysis revealed that the decrease of locomotion was significantly lower in *Rxrγ*$^{-/-}$ mice as compared to WT controls for haloperidol doses of 0.1 and 0.2 mg/kg (p < 0.05; Figure 6A). These effects of haloperidol cannot be attributed to an altered susceptibility of *Rxrγ*$^{-/-}$ mice to develop catalepsy, since a 0.2 mg/kg dose did not induce catalepsy in WT and *Rxrγ*$^{-/-}$ mice, whereas a high dose of haloperidol (2 mg/kg) induced comparable degrees of catalepsy in both genotypes (Figure 6B).

Rxrγ in the Nucleus Accumbens Is Critical for Control of Despair and Hedonic Behaviors and Modulation of D2r Expression

To investigate whether Rxrγ expression in the nucleus accumbens shell plays a role in the control of depressive-like behaviors and expression of dopamine D2r, we carried out functional rescue experiments using stereotaxic injection of adenoassociated virus (AAV2) expressing Rxrγ, in the NAc of *Rxrγ* null mutants. Using immunohistochemical analysis, we could clearly detect the expression of Rxrγ protein in the WT noninjected mice (top panels in Figure 7A) or in the NAcSh of *Rxrγ*$^{-/-}$ mice infected with AAV2-*Rxrγ* vector (bottom panels in Figure 7A), but not in *Rxrγ*$^{-/-}$ animals infected with AAV2-*Gfp* virus (middle panels in Figure 7A). The virus-mediated expression of Rxrγ in *Rxrγ*$^{-/-}$ mice was detectable bilaterally at bregma 1.1 and 1.4 and specifically in the NAcSh in 5 (out of 10) mice injected with AAV2-*Rxrγ* whereas for AAV2-*Gfp* infected mice, such pattern of Gfp expression was identified in 7 (out of 10) animals. In the

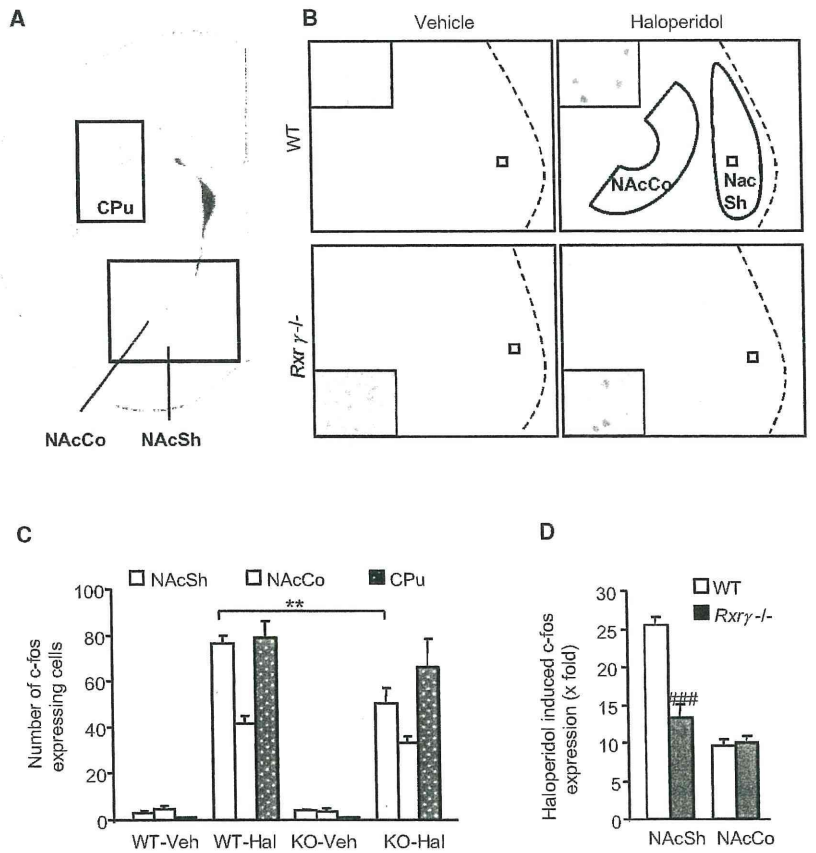

Figure 8. Haloperidol Induction of c-*fos* Expression Is Impaired in the NAc Shell of *Rxrγ*$^{-/-}$ Mutants

The brain regions used for c-*fos* counts are schematized (A). c-*fos* positive cells were scored in selected regions of the dorsal striatum (striped area; CPu) (A), the nucleus accumbens shell (NAcSh) and core (NAcCo) (B). c-*fos*-positive cells were counted for each structure and are presented as means ± SEM (C) or as the ratio of haloperidol/vehicle induced c-*fos* cells for each genotype (D). Each experimental group consisted of n = 6 animals. Data are presented as mean values ± SEM. $^{**}p < 0.01$, $^{###}p < 0.001$.

remaining animals (n = 5 for AAV2-*Rxrγ* and n = 3 for AAV2-*Gfp*) viral infection was unilateral or not restricted to the NAc (e.g., spreading into ventral septum) and these mice were excluded from the analysis of behavioral data. The infection of *Rxrγ* null mutant mice with the AAV2-*Rxrγ* expressing vector led to a significant decrease of despair behaviors ($t = 2.8$, $p < 0.05$) and anhedonia ($t = -2.7$, $p < 0.05$) as compared to *Rxrγ*$^{-/-}$ mice infected with the Gfp-expressing virus (Figures 7B and 7C). Such behavioral effects of Rxrγ expression in the NAc were not confounded by altered locomotor activity, as spontaneous locomotion in the actimetric cages or novelty induced locomotion in the open field test were comparable between the groups (Figure S3). During the sucrose preference test the total amount of liquid consumed during the testing session was not different among the groups and was on average 4.7 ± 0.4 mg/night.

In addition to reversal of behavioral deficits, re-expression of Rxrγ in the nucleus accumbens of *Rxrγ*$^{-/-}$ mice led to an increase of the number of D2r expressing neurons. In the NAc shell of *Rxrγ*$^{-/-}$ infected with AAV2-*Rxrγ* we identified 190.2 ± 11.1 D2r-positive neurons, which was significantly more than 153.2 ± 11.2 neurons in AAV2-*Gfp* infected mutant mice ($t = -2.34$, $p < 0.05$), which was also reflected by relative measures of D2v positive cell numbers with respect to adjacent CPu region (0.23 ± 0.01 for AAV2-*Rxrγ* as compared to 0.18 ± 0.01 in AAV2-*Gfp* infected *Rxrγ*$^{-/-}$ mice; $t = -3.1$, $p < 0.05$). To address whether such an increase of D2v expression in the NAcSh is relevant to depressive-like behaviors in *Rxrγ*$^{-/-}$ mice we have blocked D2r signaling in the NAcSh by bilateral infusion of the D2r antagonist raclopride (5 μg/side) in AAV2-*Rxrγ* rescued *Rxrγ*$^{-/-}$ mice. We found that blocking D2r signaling compromised antidepressant effects of AAV2-mediated re-expression of Rxrγ in *Rxrγ*$^{-/-}$ mice since such animals remained immobile in the forced swim test for 130.6 ± 13.4 s, which was significantly longer ($t = 4.1$, $p < 0.01$) than *Rxrγ*$^{-/-}$ mice which were infected with AAV2-*Rxrγ* and infused with ACSF vehicle (57.9 ± 9.7 s; Figure 7D). Although raclopride infusion into the NAc led to a slight tendency to reduce general locomotor activity as measured in the open field (Figure 7E), such reduction was not significant ($t = -0.87$, $p = 0.4$) and cannot account for increased immobility in the forced swim test.

AAV2-Mediated Expression of D2r in the Nucleus Accumbens Reverses Depressive-like Behaviors of *Rxrγ*$^{-/-}$ Mice

In order to further address the role of a reduction of D2r expression in the control of depressive-like behaviors in *Rxrγ*$^{-/-}$ mice, we increased D2r signaling in the nucleus accumbens by AAV2 mediated expression of D2r. Seven out of nine injected *Rxrγ*$^{-/-}$ mice were retained for statistical analysis as they displayed bilateral D2r expression revealed by increased number of D2r positive neurons in the NAc (210.7 ± 10.5 in AAV2-*D2r* mice as compared to 153.2 ± 11.2 in AAV2-*Gfp* infected *Rxrγ*$^{-/-}$ mice; $t = -4.3$, $p < 0.01$). The increase of D2r-positive neurons was specific to the shell of NAc and was not present in the adjacent, dorsal part of the striatum on the same sections (Figure 8A). Such expression was functionally relevant as it increased locomotor activity in the open field (Figure 8B), which attained 122.3 ± 10 m for AAV2-*D2r* mice as compared to 96.9 ± 3.7 m of distance covered by AAV2-*Gfp* mice ($t = 2.35$, $p < 0.05$). Increased activity resulted from abnormal reactivity to a novel environment and could be further demonstrated by increased

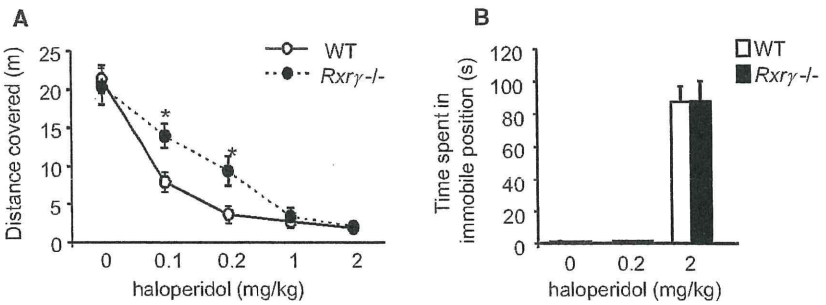

Figure 6. Behavioral Responses to Haloperidol in $Rxr\gamma^{-/-}$ Mice

Twenty minutes after treatment with saline (0) or haloperidol (0.1, 0.2, 1, or 2 mg/kg), locomotor activity was measured in WT and $Rxr\gamma^{-/-}$ mice in the open field test during 5 min. The number of animals tested in each genotype/treatment group was: $n_{WT/0} = 7$, $n_{Rxr\gamma-/-/0} = 7$, $n_{WT/0.1} = 8$, $n_{Rxr\gamma-/-/0.1} = 10$, $n_{WT/0.2} = 8$, $n_{Rxr\gamma-/-/0.2} = 7$, $n_{WT/1} = 7$, $n_{Rxr\gamma-/-/1} = 7$, $n_{WT/2} = 7$, $n_{Rxr\gamma-/-/2} = 10$ (A). Catalepsy was measured in the bar test 30 min after vehicle (0) or haloperidol (0.2 or 2mg/kg) injection (B). The number of animals tested in each genotype/treatment group was: $n_{WT/0} = 8$, $n_{Rxr\gamma-/-/0} = 8$, $n_{WT/0.2} = 10$, $n_{Rxr\gamma-/-/0.2} = 7$, $n_{WT/2} = 8$, $n_{Rxr\gamma-/-/2} = 8$. Data are presented as mean values ± SEM. *$p < 0.05$ with respect to WT haloperidol-treated group.

locomotion in the actimetric cages, which was evident during the first hr of the 32 hr test (Figure S3), thus reflecting enhanced D2r signaling (Ouagazzal and Creese, 2000; Zhang et al., 1996). In the forced swim test $Rxr\gamma^{-/-}$ mice infected with AAV2-*D2r* remained immobile for 58 ± 11.1 s, which was significantly less ($t = -3.5$, $p < 0.01$) than 127.9 ± 16.7 s for AAV2-*Gfp* mice (Figure 8C). AAV2-mediated D2r expression also normalized anhedonia of $Rxr\gamma^{-/-}$ mice. Indeed, $Rxr\gamma^{-/-}$ mice infected with AAV2-*D2r* preferred sucrose to water and consumed 73.8% ± 6.9% of sucrose as opposed to significantly lower ($t = 2.62$, $p < 0.05$), 53.3% ± 4.3% for AAV2-*Gfp* control mice (Figure 8D).

DISCUSSION

We provide here evidence that a specific retinoid receptor is implicated in the control of affective behaviors in mice. We show that null mutation of *Rxrγ* leads to increased despair behavior in the forced swim test and anhedonia, the key symptom of depression as measured in the sucrose preference paradigm. Our studies of single and compound $Rxr\gamma^{-/-}$ and $Rar\beta^{-/-}$ mutant mice provide also evidence that Rarβ might not be the heterodimerization partner of Rxrγ in control of affective behaviors. Although we cannot exclude some functional redundancy between Rar's in their interactions with Rxrγ, it is unlikely that Rarα or Rarγ, the two other Rar isotypes, may functionally compensate for the loss of Rarβ, since these receptors display very limited coexpression with Rxrγ (Krezel et al., 1999). Considering that in addition to Rar's, the Rxr's interact with other members of the nuclear receptor superfamily, the nature of the heterodimerization partner of Rxrγ remains to be determined.

The behavioral abnormalities displayed by $Rxr\gamma^{-/-}$ mice are of particular relevance for research on depression, as they resemble some of the core symptoms specific to depressive disorders and they could be reversed by chronic fluoxetine treatment. Such functions of Rxrγ are specific to central control of affective behaviors, since *Rxrγ* null mutant mice do not present dysfunction of the peripheral nervous system or muscles and with the exception of compromised working memory (Wietrzych et al., 2005), they do not display any other apparent abnormalities (Krezel et al., 1996, 1998). Thus, considering efficiency of chronic treatment with fluoxetine to reverse anhedonia and despair we speculated that abnormal serotonin signal might be at the origin of depressive-like phenotype in $Rxr\gamma^{-/-}$ mice. Although such hypothesis could be further supported by increased 5HT tissue levels in the striatum and a strong tendency ($p = 0.08$) for increased 5HT turnover in the hippocampus of knockout mice, we found that acute modulation of serotonergic signaling by single treatment with fluoxetine did not affect performance of $Rxr\gamma^{-/-}$ mice in the forced swim test, suggesting strongly that altered serotonin signaling is not sufficient to generate depressive-like behaviors in these mice. In consequence, we considered that long term, adaptive changes associated with chronic fluoxetine treatment might be relevant for beneficial effects of this antidepressant treatment and for the mechanisms of depressive-like behaviors in $Rxr\gamma^{-/-}$ mice. We investigated, therefore, dopaminergic signaling, known to be modulated by chronic fluoxetine treatment and the key neurotransmission pathway involved in the control of motivated behaviors. The dopamine D2 receptor has been suggested to be particularly relevant to such regulations, and its potential implication in depressive disorders and role in antidepressant therapies have been investigated (Dailly et al., 2004; Millan, 2006; Nestler and Carlezon, 2006). In addition, D2r is known to be a direct transcriptional target of retinoid receptors (Krezel et al., 1998; Samad et al., 1997). We found that the inactivation of Rxrγ led to a significant reduction in *D2r* mRNA expression specifically within the nucleus accumbens, whereas the expression of D1r was not affected in any part of the striatum. Interestingly, our in situ hybridization analysis suggested that reduced D2r expression may concern only a subpopulation of neurons in the shell of NAc, since in this region (1) the number of enkephaline positive neurons, a distinct marker of D2r neurons was not altered in $Rxr\gamma^{-/-}$ mice, (2) the intensity of D2r signal was not reduced in D2r positive neurons of $Rxr\gamma^{-/-}$ mice indicating that reduced D2r expression is not generalized, whereas (3) chronic fluoxetine treatment increased the number of D2r positive neurons in $Rxr\gamma^{-/-}$ mice, but not in WT mice.

At the moment, it is not clear why reduction of D2r expression was not observed in the dorsal striatum of $Rxr\gamma^{-/-}$ mice, which together with the shell of NAc are the brain regions with the most prominent expression of Rxrγ (Krezel et al., 1999). One

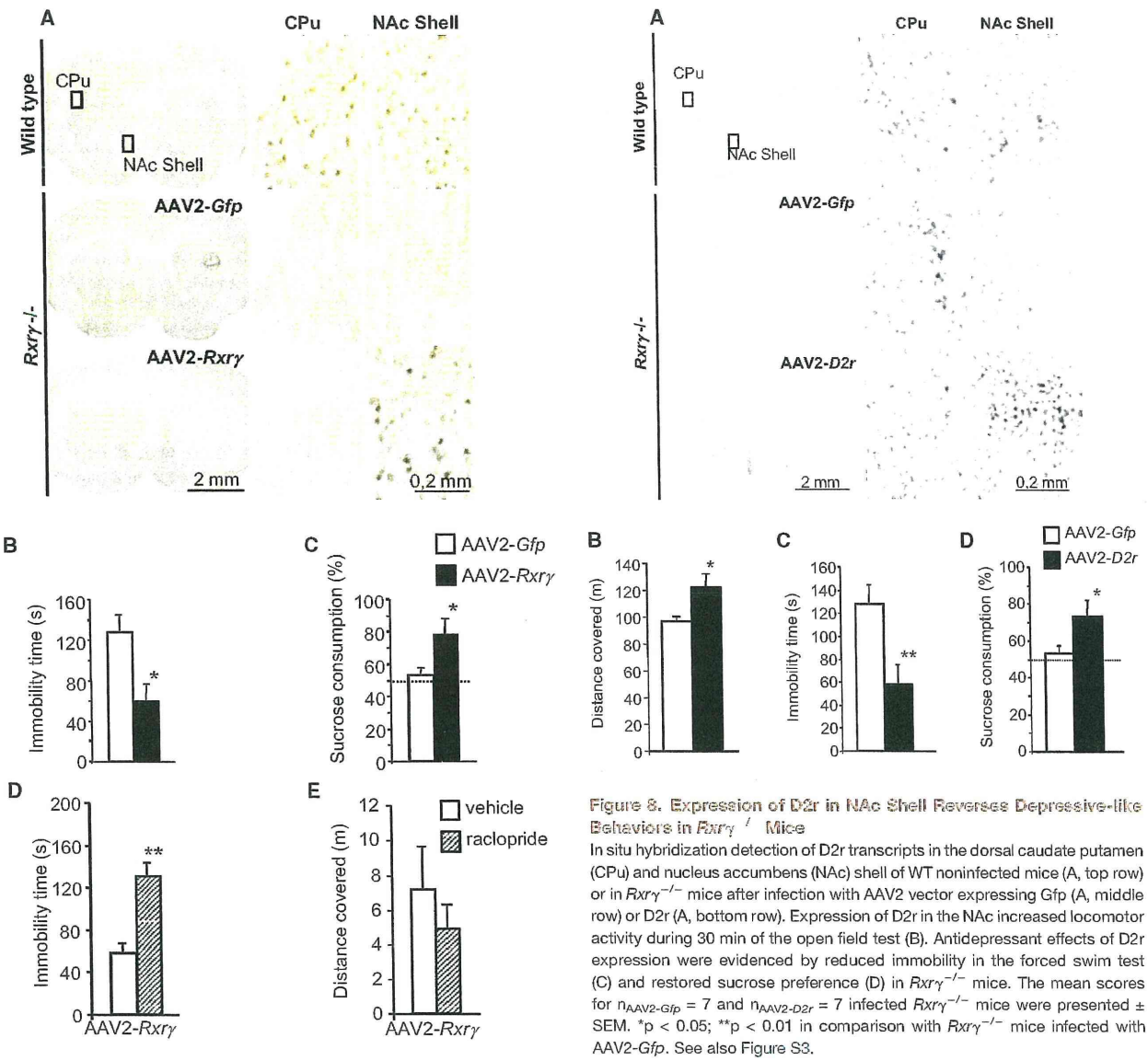

Figure 8. Expression of D2r in NAc Shell Reverses Depressive-like Behaviors in *Rxrγ*$^{-/-}$ Mice

In situ hybridization detection of D2r transcripts in the dorsal caudate putamen (CPu) and nucleus accumbens (NAc) shell of WT noninfected mice (A, top row) or in *Rxrγ*$^{-/-}$ mice after infection with AAV2 vector expressing Gfp (A, middle row) or D2r (A, bottom row). Expression of D2r in the NAc increased locomotor activity during 30 min of the open field test (B). Antidepressant effects of D2r expression were evidenced by reduced immobility in the forced swim test (C) and restored sucrose preference (D) in *Rxrγ*$^{-/-}$ mice. The mean scores for $n_{AAV2\text{-}Gfp} = 7$ and $n_{AAV2\text{-}D2r} = 7$ infected *Rxrγ*$^{-/-}$ mice were presented ± SEM. *$p < 0.05$; **$p < 0.01$ in comparison with *Rxrγ*$^{-/-}$ mice infected with AAV2-*Gfp*. See also Figure S3.

Figure 7. Re-expression of *Rxrγ* in NAc Shell Reverses Depressive-like Behaviors in *Rxrγ*$^{-/-}$ Mice through D2r-Dependent Mechanism

Immunohistochemical detection of Rxrγ in the dorsal caudate putamen (CPu) and nucleus accumbens (NAc) shell of WT noninfected mice (A, top row) or *Rxrγ*$^{-/-}$ mice after infection with AAV2 vector expressing Gfp (A, middle row) or *Rxrγ* (A, bottom row). Re-expression of *Rxrγ* in the NAc shell reduced immobility in the forced swim test (B) and restored sucrose preference (C) in $n_{Rxr\gamma-/-} = 7$ mice as compared with $n_{Rxr\gamma-/-} = 5$ mice infected with AAV2-*Gfp*. Acute inhibition of D2r signaling in the NAc shell after bilateral infusion of raclopride (5 μg/side) prevented AAV2-*Rxrγ* rescue of depressive-like behaviors in *Rxrγ*$^{-/-}$ mice as measured in the forced swim test for $n_{raclopride} = 5$ and $n_{ACSF} = 7$ infused mice (D). Locomotor activity in the open field test was studied in the same mice 2 days after forced swim test (E). Data are presented as mean values ± SEM. *$p < 0.05$ in comparison with *Rxrγ*$^{-/-}$ mice infected with AAV2-*Gfp*; **$p < 0.01$ in comparison with ACSF infused control group. See also Figure S3.

possible explanation is that transcriptional control of D2r expression in the dorsal striatum is subject to marked functional redundancy between Rxrγ and Rxrα and/or Rxrβ. Such hypothesis is supported by an overall reduction of striatal D2r expression and severe locomotor deficits displayed by *Rxrβ/Rxrγ* double null mutants, these defects being absent in the corresponding single null mutants (Krezel et al., 1998).

The reduction of *D2r* mRNA expression in the NAc of *Rxrγ*$^{-/-}$ mice is relevant for D2r functions, as we observed that c-*fos* induction by haloperidol treatment, a D2r antagonist was blunted in mutant mice. In concordance with the topography of deficits in D2r expression, reduced activation of c-*fos* expression was observed in the shell of the NAc, indicating that the reduction of D2r functions might be restricted to this region of the ventral striatum. Such observations are further supported by a blunted

locomotor response of *Rxrγ*$^{-/-}$ mice to low, noncataleptic doses of haloperidol. Thus, *Rxrγ* null mutant mice were less prone to reduction of locomotor activity in response to haloperidol treatment, suggesting compromised D2r responsiveness in the ventral striatum, the region strongly implicated in the control of horizontal locomotion (Amalric and Koob, 1993; Messier et al., 1992; Pijnenburg et al., 1976; Zhang et al., 1996).

Reduced D2r signaling in *Rxrγ*$^{-/-}$ mice might be directly related to depressive-like deficits displayed by these mice. In line with this hypothesis, we found that chronic fluoxetine reversal of depressive-like behaviors was accompanied by an increase of D2r expression in the NAcSh of *Rxrγ*$^{-/-}$ mice. To further explore the behavioral relevance of compromised D2r signaling in *Rxrγ*$^{-/-}$ mice and the implication of Rxrγ in such control, we carried out rescue experiments by virus-mediated re-expression of Rxrγ in *Rxrγ*$^{-/-}$ mice. We found that re-expression of Rxrγ in the shell of NAc is critical for modulation of D2r expression and affective behaviors. This was illustrated by an increase of the number of D2r expressing neurons in the NAc and a reversal of behavioral deficits in the forced swim and sucrose preference tests following AAV2 mediated re-expression of Rxrγ in the NAc of *Rxrγ*$^{-/-}$ mice. An increase of D2r expression in NAc appeared to play a critical role in the antidepressant-like activities of Rxrγ, since infusion of raclopride, a D2r/D3r antagonist, prevented the rescue of despair behaviors in *Rxrγ*$^{-/-}$ mice infected with AAV2-*Rxrγ*. Furthermore, we showed that a long-lasting increase of D2r signaling by AAV2 mediated expression of D2r in the NAcSh of *Rxrγ*$^{-/-}$ mice reversed both despair behaviors in the forced swim and anhedonia in the sucrose preference test. The functionality of viral expression of D2r was confirmed by an increased number of D2r neurons, but also by an increase in novelty induced locomotion as tested in the open field or actimetric cages, which is in agreement with stimulating locomotor effects D2r activation in NAc (Ouagazzal and Creese, 2000; Zhang et al., 1996). Interestingly, such increased locomotion was not observed following re-expression of Rxrγ in *Rxrγ*$^{-/-}$ mice even though it also increased expression of D2r. Such difference might be related to quantitative and qualitative differences in D2r expression, which might have been stronger and display distinct, cell type-specific activities after infection with AAV2-*D2r* as compared to mice infected with AAV2-*Rxrγ*. Although such increased activity may confound results of the forced swim test, we suggest that reduced immobility, induced by AAV2-mediated expression of D2r in *Rxrγ*$^{-/-}$ mice reflects antidepressant activities since (1) inhibition of D2r signaling by raclopride, which prevented AAV2-*Rxrγ* rescue of despair behaviors in *Rxrγ*$^{-/-}$ mice, was devoid of nonspecific behavioral effects on locomotion as measured in the open field test; (2) viral expression of D2r also normalized anhedonia in *Rxrγ*$^{-/-}$ mice, a distinct measure of depressive-like behaviors, not affected by locomotor side effects of AAV2-*D2r* infection. Finally, considering that AAV2 infections lead to low levels of retrograde transduction (Paterna et al., 2004), our data on antidepressant effects of AAV2-*D2r* infection of *Rxrγ*$^{-/-}$ mice suggest the role of postsynaptic D2r in NAc in control of affective behaviors.

In conclusion, this study provides the first evidence that the loss of Rxrγ signaling leads to depressive-like behaviors in mice and indicates that decreased dopamine D2r signaling in the shell of the NAc plays a critical role in Rxrγ control of affective behaviors. Considering that retinoids or n-3 PUFAs (de Urquiza et al., 2000; Lengqvist et al., 2004; M.W. et al., unpublished data) can modulate Rxr activities in vitro and in vivo, the present data might be of direct relevance for antidepressant activities of n-3 PUFAs reported in clinical conditions (Logan, 2004; Peet and Stokes, 2005) or depression associated with isotretinoin treatment (Bremner and McCaffery, 2008; Kontaxakis et al., 2009). In addition, mnemonic deficits specific to working memory, which were described in *Rxrγ*$^{-/-}$ mice (Wietrzych et al., 2005) might be relevant to cognitive deficits associated with depression. Such deficits, although not considered as the core symptoms of depression, are found in most forms of clinical depression. Consequently, our data suggest that Rxrγ is a potential novel target for antidepressant treatments. Unlike conventional neuropharmacology, treatments targeting retinoid receptor(s) could modulate availability of specific neurotransmitter receptors by fine, transcriptional control of their expression. Thus, Rxr ligands such as bexaroten (Targretin), used so far in cancer treatment, might be potentially interesting for clinical trials in treatment of depressive disorders.

EXPERIMENTAL PROCEDURES

Animals

Rarβ$^{-/-}$ and *Rxrγ*$^{-/-}$ single mutant, and *Rarβ*$^{-/-}$*Rxrγ*$^{-/-}$ double mutant male mice as well as their wild-type (WT) control mice were raised on a mixed genetic background (60% C57BL/6J and 40% 129SvEms/j) from heterozygous crosses as described (Krezel et al., 1996), and tested at the age of 4–5 months. All mice were housed in groups of 4–5 mice per cage in a 7 a.m.–7 p.m. light/dark cycle in individually ventilated cages, type "MICE" (Charles River, France). Food and water were freely available. All experiments were carried out in accordance with the European Community Council Directives of 24 November 1986 (86/609/EEC) and in compliance with the guidelines of CNRS and the French Agricultural and Forestry Ministry (decree 87848).

Behavioral Procedures

Forced Swim Test

The forced swim paradigm (Dalvi and Lucki, 1999) was carried out between 1 p.m. and 4 p.m. in a 2-l glass beaker half-filled with water at 22°C–23°C (the water depth was 15 cm). All mice were tested only once in this task. To this end, each mouse was lowered gently into the water and the time of immobility was scored during a 6 min testing period. The mouse was judged immobile when it floated in an upright position and made only small movements to keep its head above the water. After 6 min, the mouse was taken out of the water, left to dry under a red light lamp and returned to its home cage.

Sucrose Preference Test

This task, designed to measure hedonic behaviors in mice (Moreau, 1997; Nestler et al., 2002), is based on the palatable nature of sucrose observed in a number of mouse strains. Mice were first habituated to experimental conditions by an overnight housing in individual cages equipped with one bottle filled with water. On the first day of the test, sucrose-naive mice were placed at 5 p.m. in the same individual cages with one bottle filled with water and another with 1% sucrose solution. Three hours later (8 p.m.) the bottles were weighed to measure liquid consumption and were replaced in cages until morning to continue habituation to experimental conditions. Over 2 additional days, animals were further habituated to sucrose solution in their home cages. The measures of an overnight consumption were then carried out from 5 p.m. until 8 a.m. to evaluate sucrose preference. Mice were not water deprived at any moment, in order to measure spontaneous sucrose preference and exclude any potential emotional confounds induced by stress of water

deprivation. The sucrose preference was expressed as the percent of sucrose solution consumed with respect to total liquid consumption.

Actimetry

Spontaneous activity was measured in actimetric cages (Immetronic, Pessac, France) with the help of two arrays of infrared beam photo-cells installed on the side walls in each individual cage. Mice were placed in actimetric cages at 11 a.m. and their activity was recorded over 32 hr including a habituation period between 11 a.m. and 7 p.m. and a complete dark/light cycle until 7 p.m. of the next day.

Open Field

Mice were tested in parallel in five automated open-fields (44.3 × 44.3 × 16.8 cm) made of PVC with transparent walls and a black floor, covered with transparent PVC (Panlab, Barcelona, Spain). The open fields were placed in a room homogeneously illuminated at 150 Lux. Unless otherwise specified each mouse was placed in the periphery of the open field and allowed to explore freely the apparatus for 30 min, with the experimenter out of the animal's sight. Activity parameters including distance traveled over the test session were calculated automatically.

Catalepsy Test

Mice were injected intraperitoneally with 0.2 or 2 mg/kg of haloperidol (Sigma) and after 30 min were placed in the test cage with their forelimbs on the wooden transversal bar fixed at a level of 3 cm above floor level. The latency to move out from the bar was scored and used as index of catalepsy.

Production and Use of Adenoassociated Virus (AAV) Vectors

For generation of AAV vectors we used a vector plasmid containing an expression cassette, in which a human cytomegalovirus immediate-early promoter (CMV promoter) was followed by the first intron of the human growth hormone gene, the cDNA of interest, woodchuck hepatitis virus posttranscriptional regulatory element (WRPE; nucleotides 1093 to 1684, GenBank accession number J04514) and simian virus 40 polyadenylation signal sequence. This expression cassette was inserted between the inverted terminal repeats (ITR) of the AAV-2 genome as described (Li et al., 2006). The viral vectors used for expression of *Rxrγ* (AAV2-*Rxrγ*), *D2r* (AAV2-*D2r*), and *EGfp* (AAV2-*Gfp*) contained the entire cDNA sequences of *Rxrγ* (GenBank accession number NM_009107), *D2r* (long isoform, GenBank accession number NM_010077.2), or *EGfp*, respectively. We used two helper plasmids, pAAV-*RC* and pHelper, harboring the AAV *rep* and *cap* genes, and the *E2A*, *E4*, *VA1* genes of the adenovirus genome, respectively (Agilent Technologies, Santa Clara, CA). HEK293 cells were cotransfected with pAAV-*RC* and pHelper plasmids using the calcium phosphate coprecipitation method. AAV particles were then harvested and purified by two sequential continuous iodoxale ultracentrifugations. The vector titer was determined by quantitative PCR of DNase-I-treated vector stocks, and were estimated at 10^{10} to 10^{12} vector genome copies (vg).

For rescue experiments and D2r expression we used behaviorally naive $Rxr\gamma^{-/-}$ male mice (n = 29) at the age of 8 months. Each animal was anaesthetized using ketamine (100 mg/kg)/xylasine (10 mg/kg) solution and 0.7 μl of AAV2-*Rxrγ*, AAV2-*D2r*, or AAV2-*Gfp* suspension was injected bilaterally into the nucleus accumbens (bregma = +1.5; lateral = ±0.7; ventral = +4.2, the coordinates identified prior to experiments using dye injections and corresponding to bregma = + 1.3; lateral = ±0.5; ventral = +4.0 position in the Mouse Brain Atlas; Paxinos and Franklin, 2001) using a stereotaxic apparatus (Precision Cinematographique, Paris, France). The injection was carried out at 50 nl/min using a Harvard Apparatus PHD 2000 pump (Holliston, USA), and the injectors were withdrawn from the brain 20 min after the end of the injection. After placing stitches each animal was left to awake in the temperature-conditioned cage. Mice were tested 4 weeks later and their brains were removed for post hoc analyses.

Drug Infusion Procedure

$Rxr\gamma^{-/-}$ mice (n = 15) aged between 4 and 5 months were infected with AAV2-*Rxrγ* as described. Four weeks later, mice were anaesthetized with ketamine/xylazine solution and 8 mm long stainless-steel guide cannulas (0.4 mm external diameter; Cortat, Courrendlin, Switzerland), were positioned bilaterally 1 mm above the NAcSh (bregma = +1.5; lateral = ±0.7; ventral = +3.2) using stereotaxic apparatus (Precision Cinematographique, Paris, France). The cannulas were fixed to the skull with anchoring screws and dental cement. Stainless steel stylet rods were inserted into the cannulas to prevent occlusion. On the day of the experiment raclopride (a D2/D3 specific antagonist soluble in aqueous solutions; Sigma) was dissolved in fresh artificial cerebrospinal fluid (ACSF, which consisted of 3 mM KCl, 140 mM NaCl, 2 mM glucose, 1.2 mM $CaCl_2$, 1 mM $MgCl_2$, 0.27 mM NaH_2PO_4, 1.2 mM Na_2HPO_4 [pH 7.4]) and infusions of 0.25μl of raclopride (5 μg/side) or vehicle (ACSF) were performed at 100 nl/min using Harvard Apparatus PHD 2000 pump and stainless-steel injector needles (0.28 mm external diameter) that protruded from the cannula by 1 mm, into the NAcSh. Three minutes after injection injector needles were removed from the brain, the stylet rods were replaced in cannula guides and mice were transferred to their home cage for 5 min prior to the forced swim test. Forty-eight hours later, mice were semirandomly infused with raclopride or ACSF to test the locomotor effects of such treatments. For this experiment mice were placed in the open field immediately after removing injectors and placement of stylet rods and their activity was scored 5 min later during 5 min. Three out of fifteen mice were excluded from analysis due to unilateral AAV2-*Rxrγ* infection or incorrect guide placement, and two mice could not be infused for the open field test since the stylets remained blocked.

Pharmacological Treatments

Haloperidol (Sigma-Aldrich) was dissolved in acetic acid solution and pH was neutralized with NaOH. For c-*fos* expression studies, mice were injected intraperitoneally (IP) with saline or 1 mg/kg of haloperidol, 90 min prior to sacrifice, whereas for analysis of the open field behavior saline or haloperidol were injected 20 min prior to the test and animals were tested for 10 min. IP injection was also used for acute fluoxetine (Lilly France) treatment 30 min prior to forced swim test. For chronic treatment, fluoxetine was added to the standard chow diet. Accordingly, we supplemented standard chow in powdered form with fluoxetine to attain the dose of 20 mg of fluoxetine per kg of body weight during 24 hr. To calculate such a dose, the food consumption was first estimated experimentally to be 4 g of food pellets per 24 hr per animal. Fluoxetine-supplemented food pellets were immediately lyophilized and stored at −20°C until use. For treatment, standard chow pellets were replaced by fluoxetine-supplemented food pellets and were provided ad libitum in standard home cages throughout treatment period. The consumption of fluoxetine-containing pellets did not differ from the consumption of nonsupplemented food pellets in control cages. WT and $Rxr\gamma^{-/-}$ mice treated with fluoxetine or fed control diet were all tested for sucrose preference on the nineteenth day of treatment, and in the forced swim test on the twenty-first day of treatment, with the exception of mice used for evaluation of fluoxetine effects on D2r expression, which were all behaviorally naive.

Quantitative RT-PCR

Dissection of Brain Areas

Mice were killed by cervical dislocation. Whole brains were extracted, fresh-frozen in OCT, and kept at −80°C until use. Tissue corresponding to the nucleus accumbens (NAc) was collected with 0.5 mm punch from three subsequent 300 μm thick cryosections. Similarly, dorsolateral striatum (CPu) was collected using 0.8 mm punch from four subsequent frozen sections of 300 μm. The accurate location of these brain structures was based on visual inspection of each section using a stereomicroscope (Leica, Wild M715) and its comparison with the stereotaxic atlas of mouse brain; Paxinos and Franklin, 2001). Tissue samples were placed on dry ice and kept at −80°C until use.

Quantitative RT-PCR

Total RNA extraction was carried out using the RNeasy Micro Kit protocol (QIAGEN, France). Total RNA from each tissue sample was transcribed into cDNA using QuantiTect Reverse Transcription Kit according to the manufacturer's recommendation. Briefly, the reaction was carried out at 42°C for 20min in a total volume of 20 μl and was inactivated at 95°C. Twenty-times-diluted cDNA was used as a template, and quantitative real-time PCR was run in a LightCycler 480 (Roche, Diagnostics, Mannheim, Germany) using LightCycler SYBR Green kit (Roche, Diagnostics) with cDNA and gene-specific primers (100 μM) following the manufacturer's instructions. All of the reactions were performed in triplicate with the following cycling

protocol: 10 min of heat activation of the enzyme at 95°C, 45 cycles of denaturation at 95°C for 5 s, annealing at 60°C for 30 s, and extension at 72°C for 20 s. Fluorescence detection was performed at 72°C. Gene-specific primers were designed using Primer3 software (primer3) to amplify fragments of 150–250 bp as follows: for *D2r* (Drd2; NM 010077) forward, TCGCC ATTGTCTGGGTCCTG; reverse, TGCCCTTGAGTGGTGTCTTC; *D1r* (Drd1a; NM 010076) forward, AAGATGCCGAGGATGACAAC; reverse, CCCTC TCCAAAGCTGAGATG. The transcript amounts evaluated for *D1r* and *D2r* were normalized for the quantity and quality of each sample by division by the amount of transcript of the housekeeping gene acidic ribosomal phosphoprotein P0 (Arbp or 36B4; NM 007475) in the same sample and such relative values were presented in Figures 4A and 2S. *36B4* transcript amount was quantified using forward primer ACCCTGAAGTGCTCGACATC and reverse primer AGGAAGGCCTTGACCTTTTC.

In Situ Hybridization and Analysis of Expression Levels

In situ hybridization (ISH) was performed on 14 μm thick frozen sections with digoxigenin-labeled riboprobes synthesized from a 1680 bp *D2r* cDNA template and an enkephaline 800 bp cDNA template as described (Krezel et al., 1998). Hybridization conditions were as described previously (Krezel et al., 1998) and are available on the http://empress.har.mrc.ac.uk/ website. The amount of probe used for hybridization and signal detection conditions was adapted to avoid saturation of the chromogenic labeling (see below). Expression patterns were documented using a macroscope (Leica M420) or microscope (DM4000B), both connected to a Photometrics camera with the CoolSNAP (v. 1.2) software (Roger Scientific, Chicago, IL).

For the analysis of cell counts and expression levels of D2r, the images were transformed into gray scale and analyzed using ImageJ software (Rasband, 1997). The strongest signal observed for any of the neurons in any of the brain sections remained between 67 and 95 units in a 0 to 255 unit gray scale (0 corresponding to black), being thus 25%–30% below full saturation conditions in order to enable quantitative analysis of signal intensity. For each animal, the cell number and intensity of cellular signal was evaluated within selected regions of CPu, NAcSh and NAcCo on the same sections (for region selection see Figures 5A and 5B) at bregma 1.10 and 1.40 (Paxinos and Franklin, 2001). The mean values of cell counts or intensity for each region were calculated and compared as described in Results.

Immunohistochemistry and c-*fos* Cell Counts

Coronal sections (14 μm thick) from unfixed frozen brains of 4-month-old *Rxrγ*$^{-/-}$ mice and their WT littermates were collected on super-frost slides and stored at −80°C until analysis. Sections were postfixed in 4% paraformaldehyde and treated with 1% H_2O_2 to block endogenous peroxides. For detection of Rxrγ, we used rabbit anti-Rxrγ polyclonal antibody (SC555, batch A111, Santa Cruz, US), whereas c-*fos* was detected using rabbit anti-c-*fos* polyclonal antibody (1:1000, Chemicon). Both primary antibodies were detected using the ABC system (Vector, USA) according to the manufacturer's manual. For each animal and section, corresponding brain regions were identified according to the mouse brain atlas (Paxinos and Franklin, 2001) and c-*fos*-positive cells were counted from identical surfaces defined by region-corresponding auto-shape figures (Figures 5A and 5B) at two levels of the striatum (bregma 1.10 and 1.40; Mouse Brain Atlas; Paxinos and Franklin, 2001). The mean cell counts for each brain region were calculated and compared as described in Results.

HPLC Measures of Serotonin and Its Metabolites in the Brain Tissue

The brain samples of n = 6 WT and n = 6 *Rxrγ*$^{-/-}$ male littermates (4months old) were weighed immediately after collection and frozen at −80°C until use. Before analysis, samples were thawed, and homogenized in 10 volumes (w/v) of 0.1 M $HClO_4$ containing the internal standard DHBA (125ng/ml). The homogenates were centrifuged at 12.000 rpm for 20 min at 4°C and supernatant was retained for analysis. Serotonin and its metabolite 5-hydroxyindoleacetic acid (5HIAA) were evaluated using high performance liquid chromatography (HPLC) with electrochemical detection. The chromatographic system consisted of a 25 cm × 4.6 mm Hypersyl C18 ODS column (particle size 5μm, Biochrom, France). The column was kept at a constant temperature of 30°C. The flow rate was 1.2 ml/min with a back pressure of 1500 psi (Waters Instrumentation). The system was linked to a Waters model 460 electrochemical detector with a glassy-carbon electrode. Detector potential was maintained at 0.85 V (reference, Ag/AgCl electrode). The mobile phase consisted of 0.05 M NaH_2PO_4 and 0.1 mM EDTA (pH adjusted to 4.85 with NaOH) in double-distilled water with methanol (6%). The system was calibrated by injecting various amounts (3.4 pg–34 ng) of standard solutions, containing 1.1 ng of internal standard DHBA (3–4 dihydroxybenzylamine 1 mM in $HClO_4$ 0.1 M). The supernatant of each sample was injected onto the column, and peak identification was performed by comparing retention times with the calibration solution. Results were expressed in ng/g ±SEM.

Statistical Analysis

The comparisons of behavioral performance in *Rarβ*$^{-/-}$/*Rxrγ*$^{-/-}$, *Rarβ*$^{-/-}$, and *Rxrγ*$^{-/-}$ null mutant mice were carried out using the protected least significant difference (PLSD) Fischer test. The pharmacological data for the treatments in WT and *Rxrγ*$^{-/-}$ mice were analyzed using two-way analysis of variance (ANOVA)—with treatment and genotype as two independent factors and behavioral responses as dependent variables. Comparison of the evolution of locomotor performance in the open field or actimetric cages were evaluated using ANOVA on repeated-measures. Global and post hoc statistical analyses were performed using the PLSD Fischer test and for two-group comparisons using student t test (see t values in the text). Significant differences are indicated in the corresponding figures.

SUPPLEMENTAL INFORMATION

Supplemental Information includes three figures and can be found with this article online at doi:10.1016/j.neuron.2010.05.004.

ACKNOWLEDGMENTS

We thank Chaouki Bam'Hamed and Raphael Bour for excellent animal care, Naomi Takino, Hitomi Miyauchi, Keiko Ayabe for their help with producing AAV-vectors and Mme Carmen Schleef for expert help in HPLC analysis, and Eric Nestler, Pierre Chambon, Abdel-Mouttalib Ouagazzal and Pascal Dollé for critical reading of the manuscript. A.K. was supported by a PhD fellowship of the French Embassy in Poland and ANR grant "Neuroprotect and is a member of European Doctoral College in Strasbourg, M.S.-N. by the Association pour la Recherche sur le Cancer, M.W. by a fellowship from the Fondation pour la Recherche Médicale. This work was supported by funds from the Institut National de la Santé et de la Recherche Médicale (INSERM), the Centre National de la Recherche Scientifique (CNRS), the Institut Clinique de la Souris (ICS), and grants from the Ministry of Education, Culture, Sports, Science, and Technology of Japan and from the Ministry of Health, Labour and Welfare of Japan.

Accepted: April 30, 2010
Published: June 23, 2010

REFERENCES

Ainsworth, K., Smith, S.E., Zetterström, T.S., Pei, Q., Franklin, M., and Sharp, T. (1998). Effect of antidepressant drugs on dopamine D1 and D2 receptor expression and dopamine release in the nucleus accumbens of the rat. Psychopharmacology (Berl.) *140*, 470–477.

Amalric, M., and Koob, G.F. (1993). Functionally selective neurochemical afferents and efferents of the mesocorticolimbic and nigrostriatal dopamine system. Prog. Brain Res. *99*, 209–226.

Blier, P., and Ward, N.M. (2003). Is there a role for 5-HT1A agonists in the treatment of depression? Biol. Psychiatry *53*, 193–203.

Blier, P., Piñeyro, G., el Mansari, M., Bergeron, R., and de Montigny, C. (1998). Role of somatodendritic 5-HT autoreceptors in modulating 5-HT neurotransmission. Ann. N Y Acad. Sci. *861*, 204–216.

Bremner, J.D., and McCaffery, P. (2008). The neurobiology of retinoic acid in affective disorders. Prog. Neuropsychopharmacol. Biol. Psychiatry *32*, 315–331.

Brocco, M., Dekeyne, A., Papp, M., and Millan, M.J. (2006). Antidepressant-like properties of the anti-Parkinson agent, piribedil, in rodents: mediation by dopamine D2 receptors. Behav. Pharmacol. *17*, 559–572.

Carlezon, W.A., Jr., Mague, S.D., Parow, A.M., Stoll, A.L., Cohen, B.M., and Renshaw, P.F. (2005). Antidepressant-like effects of uridine and omega-3 fatty acids are potentiated by combined treatment in rats. Biol. Psychiatry *57*, 343–350.

Corrigan, M.H., Denahan, A.Q., Wright, C.E., Ragual, R.J., and Evans, D.L. (2000). Comparison of pramipexole, fluoxetine, and placebo in patients with major depression. Depress. Anxiety *11*, 58–65.

Dailly, E., Chenu, F., Renard, C.E., and Bourin, M. (2004). Dopamine, depression and antidepressants. Fundam. Clin. Pharmacol. *18*, 601–607.

Dalvi, A., and Lucki, I. (1999). Murine models of depression. Psychopharmacology (Berl.) *147*, 14–16.

de Urquiza, A.M., Liu, S., Sjöberg, M., Zetterström, R.H., Griffiths, W., Sjövall, J., and Perlmann, T. (2000). Docosahexaenoic acid, a ligand for the retinoid X receptor in mouse brain. Science *290*, 2140–2144.

Dulawa, S.C., Holick, K.A., Gundersen, B., and Hen, R. (2004). Effects of chronic fluoxetine in animal models of anxiety and depression. Neuropsychopharmacology *29*, 1321–1330.

Dziedzicka-Wasylewska, M., Rogoz, R., Klimek, V., and Maj, J. (1997). Repeated administration of antidepressant drugs affects the levels of mRNA coding for D1 and D2 dopamine receptors in the rat brain. J. Neural Transm. *104*, 515–524.

Foley, K.F., DeSanty, K.P., and Kast, R.E. (2006). Bupropion: pharmacology and therapeutic applications. Expert Rev. Neurother. *6*, 1249–1265.

Kastner, P., Mark, M., Ghyselinck, N., Krezel, W., Dupé, V., Grondona, J.M., and Chambon, P. (1997). Genetic evidence that the retinoid signal is transduced by heterodimeric Rxr/Rar functional units during mouse development. Development *124*, 313–326.

Kontaxakis, V.P., Skourides, D., Ferentinos, P., Havaki-Kontaxaki, B.J., and Papadimitriou, G.N. (2009). Isotretinoin and psychopathology: a review. Ann. Gen. Psychiatry *8*, 2.

Krezel, W., Dupé, V., Mark, M., Dierich, A., Kastner, P., and Chambon, P. (1996). Rxr gamma null mice are apparently normal and compound Rxr alpha +/-/Rxr beta -/-/Rxr gamma -/- mutant mice are viable. Proc. Natl. Acad. Sci. USA *93*, 9010–9014.

Krezel, W., Ghyselinck, N., Samad, T.A., Dupé, V., Kastner, P., Borrelli, E., and Chambon, P. (1998). Impaired locomotion and dopamine signaling in retinoid receptor mutant mice. Science *279*, 863–867.

Krezel, W., Kastner, P., and Chambon, P. (1999). Differential expression of retinoid receptors in the adult mouse central nervous system. Neuroscience *89*, 1291–1300.

Larisch, R., Klimke, A., Vosberg, H., Löffler, S., Gaebel, W., and Müller-Gärtner, H.W. (1997). In vivo evidence for the involvement of dopamine-D2 receptors in striatum and anterior cingulate gyrus in major depression. Neuroimage *5*, 251–260.

Lechin, F., van der Dijs, B., and Hernandez-Adrian, G. (2006). Dorsal raphe vs. median raphe serotonergic antagonism. Anatomical, physiological, behavioral, neuroendocrinological, neuropharmacological and clinical evidences: relevance for neuropharmacological therapy. Prog. Neuropsychopharmacol. Biol. Psychiatry *30*, 565–585.

Lengqvist, J., Mata De Urquiza, A., Bergman, A.C., Willson, T.M., Sjövall, J., Perlmann, T., and Griffiths, W.J. (2004). Polyunsaturated fatty acids including docosahexaenoic and arachidonic acid bind to the retinoid X receptor alpha ligand-binding domain. Mol. Cell. Proteomics *3*, 692–703.

Li, X.G., Okada, T., Kodera, M., Nara, Y., Takino, N., Muramatsu, C., Ikeguchi, K., Urano, F., Ichinose, H., Metzger, D., et al. (2006). Viral-mediated temporally controlled dopamine production in a rat model of Parkinson disease. Mol. Ther. *13*, 160–166.

Logan, A.C. (2004). Omega-3 fatty acids and major depression: a primer for the mental health professional. Lipids Health Dis. *3*, 25.

Lucki, I., Dalvi, A., and Mayorga, A.J. (2001). Sensitivity to the effects of pharmacologically selective antidepressants in different strains of mice. Psychopharmacology *155*, 315–322.

Mattes, J.A. (1997). Pergolide to augment the effectiveness of antidepressants: clinical experience and a small double-blind study. Ann. Clin. Psychiatry *9*, 87–88.

Messier, C., Mrabet, O., and Destrade, C. (1992). Locomotor bias produced by intra-accumbens injection of dopamine agonists and antagonists. Pharmacol. Biochem. Behav. *41*, 177–182.

Millan, M.J. (2006). Multi-target strategies for the improved treatment of depressive states: Conceptual foundations and neuronal substrates, drug discovery and therapeutic application. Pharmacol. Ther. *110*, 135–370.

Millan, M.J., Seguin, L., Gobert, A., Cussac, D., and Brocco, M. (2004). The role of dopamine D3 compared with D2 receptors in the control of locomotor activity: a combined behavioural and neurochemical analysis with novel, selective antagonists in rats. Psychopharmacology (Berl.) *174*, 341–357.

Moreau, J.L. (1997). Reliable monitoring of hedonic deficits in the chronic mild stress model of depression. Psychopharmacology (Berl.) *134*, 357–358.

Naliwaiko, K., Araújo, R.L., da Fonseca, R.V., Castilho, J.C., Andreatini, R., Bellissimo, M.I., Oliveira, B.H., Martins, E.F., Curi, R., Fernandes, L.C., and Ferraz, A.C. (2004). Effects of fish oil on the central nervous system: a new potential antidepressant? Nutr. Neurosci. *7*, 91–99.

Nestler, E.J., and Carlezon, W.A., Jr. (2006). The mesolimbic dopamine reward circuit in depression. Biol. Psychiatry *59*, 1151–1159.

Nestler, E.J., Gould, E., Manji, H., Buncan, M., Duman, R.S., Greshenfeld, H.K., Hen, R., Koester, S., Lederhendler, I., Meaney, M., et al. (2002). Preclinical models: status of basic research in depression. Biol. Psychiatry *52*, 503–528.

Ouagazzal, A.M., and Creese, I. (2000). Intra-accumbens infusion of D(3) receptor agonists reduces spontaneous and dopamine-induced locomotion. Pharmacol. Biochem. Behav. *67*, 637–645.

Paterna, J.C., Feldon, J., and Büeler, H. (2004). Transduction profiles of recombinant adeno-associated virus vectors derived from serotypes 2 and 5 in the nigrostriatal system of rats. J. Virol. *78*, 6808–6817.

Paxinos, G., and Franklin, K.B.J. (2001). The Mouse Brain in Stereotaxic Coordinates (San Diego, CA: Academic Press).

Peet, M., and Stokes, C. (2005). Omega-3 fatty acids in the treatment of psychiatric disorders. Drugs *65*, 1051–1059.

Pijnenburg, A.J., Honig, W.M., Van der Heyden, J.A., and Van Rossum, J.M. (1976). Effects of chemical stimulation of the mesolimbic dopamine system upon locomotor activity. Eur. J. Pharmacol. *35*, 45–58.

Rasband, W.S. (1997). ImageJ, U. S. National Institutes of Health, Bethesda, Maryland, USA, http://rsb.info.nih.gov/ij/, 1997–2009.

Renard, C.E., Fiocco, A.J., Clenet, F., Hascoet, M., and Bourin, M. (2001). Is dopamine implicated in the antidepressant-like effects of selective serotonin reuptake inhibitors in the mouse forced swimming test? Psychopharmacology (Berl.) *159*, 42–50.

Samad, T.A., Krezel, W., Chambon, P., and Borrelli, E. (1997). Regulation of dopaminergic pathways by retinoids: activation of the D2 receptor promoter by members of the retinoic acid receptor-retinoid X receptor family. Proc. Natl. Acad. Sci. USA *94*, 14349–14354.

Siuciak, J.A., and Fujiwara, R.A. (2004). The activity of pramipexole in the mouse forced swim test is mediated by D2 rather than D3 receptors. Psychopharmacology (Berl.) *175*, 163–169.

Theohar, C., Fischer-Cornelssen, K., Brosch, H., Fischer, E.K., and Petrovic, D. (1982). A comparative, multicenter trial between bromocriptine and amitriptyline in the treatment of endogenous depression. Arzneimittelforschung *32*, 783–787.

Valentini, V., Frau, R., and Di Chiara, G. (2004). Noradrenaline transporter blockers raise extracellular dopamine in medial prefrontal but not parietal and occipital cortex: differences with mianserin and clozapine. J. Neurochem. *88*, 917–927.

Wietrzych, M., Meziane, H., Sutter, A., Ghyselinck, N., Chapman, P.F., Chambon, P., and Krezel, W. (2005). Working memory deficits in retinoid X receptor gamma-deficient mice. Learn. Mem. *12*, 318–326.

Willner, P. (1997). The mesolimbic dopamine system as a target for rapid antidepressant action. Int. Clin. Psychopharmacol. *12* (*Suppl 3*), S7–S14.

Willner, P., Hale, A.S., and Argyropoulos, S. (2005). Dopaminergic mechanism of antidepressant action in depressed patients. J. Affect. Disord. *86*, 37–45.

Zetterström, R.H., Lindqvist, E., Mata de Urquiza, A., Tomac, A., Eriksson, U., Perlmann, T., and Olson, L. (1999). Role of retinoids in the CNS: differential expression of retinoid binding proteins and receptors and evidence for presence of retinoic acid. Eur. J. Neurosci. *11*, 407–416.

Zhang, M., Ouagazzal, A., Sun, B., and Creese, I. (1996). Regulation of Motor Behavior by Dopamine Receptor Subtypes: An Antisense Knockout Approach (New Jersey: Humana Press).

A Phase I Study of Aromatic L-Amino Acid Decarboxylase Gene Therapy for Parkinson's Disease

Shin-ichi Muramatsu[1], Ken-ichi Fujimoto[1], Seiya Kato[2], Hiroaki Mizukami[3], Sayaka Asari[1], Kunihiko Ikeguchi[1], Tadataka Kawakami[1], Masashi Urabe[3], Akihiro Kume[3], Toshihiko Sato[4], Eiju Watanabe[2], Keiya Ozawa[3] and Imaharu Nakano[1]

[1]Division of Neurology, Department of Medicine, Jichi Medical University, Tochigi, Japan; [2]Department of Neurosurgery, Jichi Medical University, Tochigi, Japan; [3]Division of Genetic Therapeutics, Center for Molecular Medicine, Jichi Medical University, Tochigi, Japan; [4]Utsunomiya Central Clinic, Tochigi, Japan

Gene transfer of dopamine-synthesizing enzymes into the striatal neurons has led to behavioral recovery in animal models of Parkinson's disease (PD). We evaluated the safety, tolerability, and potential efficacy of adeno-associated virus (AAV) vector–mediated gene delivery of aromatic L-amino acid decarboxylase (AADC) into the putamen of PD patients. Six PD patients were evaluated at baseline and at 6 months, using multiple measures, including the Unified Parkinson's Disease Rating Scale (UPDRS), motor state diaries, and positron emission tomography (PET) with 6-[^{18}F]fluoro-L-*m*-tyrosine (FMT), a tracer for AADC. The short-duration response to levodopa was measured in three patients. The procedure was well tolerated. Six months after surgery, motor functions in the OFF-medication state improved an average of 46% based on the UPDRS scores, without apparent changes in the short-duration response to levodopa. PET revealed a 56% increase in FMT activity, which persisted up to 96 weeks. Our findings provide class IV evidence regarding the safety and efficacy of AADC gene therapy and warrant further evaluation in a randomized, controlled, phase 2 setting.

Received 25 January 2010; accepted 5 June 2010; published online 6 July 2010. doi:10.1038/mt.2010.135

INTRODUCTION

Dopamine replacement has been the standard pharmacotherapy for motor impairment in Parkinson's disease (PD). Although virtually all patients benefit from levodopa at an early stage of the disease, severe loss of nigrostriatal nerve terminals in advanced PD leads to profoundly decreased activities of dopamine-synthesizing enzymes, including aromatic L-amino acid decarboxylase (AADC), an essential enzyme that converts levodopa to dopamine. Failure to respond to levodopa therapy may result from a reduction in AADC activity, decreased dopamine storage capacity in synaptic vesicles, postsynaptic changes in striatal output neurons, and abnormalities of nondopaminergic neurotransmitter systems.[1,2] Systemic administration of high-dose levodopa enhances oscillations in motor performance and complications, including hallucinations, due to dopaminergic stimulation of the mesolimbic system.

One potential treatment for advanced PD is gene therapy to restore striatum-selective dopamine production. In addition to AADC, tyrosine hydroxylase, which converts L-tyrosine to levodopa, and guanosine triphosphate cyclohydrolase I, which catalyzes biosynthesis of the essential tyrosine hydroxylase cofactor, tetrahydrobiopterine, are necessary for efficient synthesis of dopamine.[2] Viral vector–mediated gene transfer of these dopamine-synthesizing enzymes has been shown to achieve behavioral recovery in animal PD models, with efficient transduction of striatal neurons that escape degeneration.[3–6] When tyrosine hydroxylase and guanosine triphosphate cyclohydrolase I are expressed in the striatum, levodopa can be synthesized continuously. This strategy would be useful for reducing motor fluctuations associated with intermittent levodopa intake. Gene transfer of AADC alone in combination with oral levodopa administration would be a safer strategy for initial clinical trials. In the latter approach, the patients still need to take levodopa to control motor symptoms, but excess production of dopamine could be avoided by reducing the dose of levodopa. We assessed the safety, tolerability, and the potential efficacy of intraputaminal infusion of recombinant adeno-associated virus (AAV) serotype 2 vector encoding human AADC (AAV-hAADC-2) in patients with mid- to late-stage PD. We also examined whether the short-duration response to levodopa, the antiparkinsonian response that parallels the plasma levodopa levels, would change after gene therapy.[7]

RESULTS

Patient disposition and baseline characteristics

Six patients (4 men, 2 women), mean age 60 (range, 51–68) years, were enrolled (Table 1). The mean disease duration was 10 (range, 5–18) years, and time on levodopa was 9.3 (range, 5–15) years. The average baseline daily levodopa and levodopa equivalent doses were 642 and 808 mg, respectively.

Correspondence: Shin-ichi Muramatsu, Division of Neurology, Department of Medicine, Jichi Medical University, 3311-1 Yakushiji, Shimotsuke, Tochigi 329-0498, Japan. E-mail: muramats@jichi.ac.jp or Imaharu Nakano, Division of Neurology, Department of Medicine, Jichi Medical University, 3311-1 Yakushiji, Shimotsuke, Tochigi 329-0498, Japan. E-mail: inakano@jichi.ac.jp

Table 1 Patients' baseline characteristics

Subject	Age (years)	Sex	Disease duration (years)	Time on levodopa (years)	Levodopa dose (mg)	Levodopa equivalents (mg)
A-1	51	M	11	9	600	900
A-2	63	M	9	9	450	650
A-3	66	F	7	7	500	700
A-4	58	M	11	11	700	700
A-5	68	F	18	15	1,000	1,100
A-6	56	M	5	5	600	800
Mean (SD)	60 (6.5)	67% M	10 (4.5)	9.3 (3.4)	642 (196)	808 (169)

Abbreviations: F, female; M, male.
Patients are listed in the order in which they received treatment. Levodopa equivalents were estimated as follows: 100 mg of levodopa with a dopa-decarboxylase inhibitor is equivalent to 0.8 mg talipexole, 1 mg pergolide, 1 mg pramipexole, and 1.5 mg cabergoline.

Primary end point

The procedure was well tolerated. All patients completed all protocol-defined visits. One patient (patient A-2) had a venous hemorrhage in the right frontal lobe just below a burr hole that was found on CT scan 3 days after infusion. The patient used his left arm less frequently than his right arm for 3 weeks; this was assumed to reflect mild frontal lobe dysfunction and resolved completely. Mild, transient headache around the burr holes was present for 2 days after surgery in all patients. There were no significant laboratory test abnormalities. All patients had mildly increased titers of anti-AAV2-neutralizing antibodies 6 months after treatment, which tended toward baseline concentrations thereafter (Table 2).

Table 2 Changes in neutralizing AAV2 antibody titers in sera following gene therapy

Subject	Pre	2 weeks	6 months	1 year
A-1	1:2	1:4	1:4	1:4
A-2	<1	1:32	1:4	1:2
A-3	1:32	1:64	1:64	1:32
A-4	1:32	1:32	1:256	1:64
A-5	1:4	1:32	1:32	1:32
A-6	<1	1:16	1:32	1:32

Abbreviations: AAV, adeno-associated virus.
Titers are determined by *in vitro* assay and represented as "1:" dilutions.

Clinical evaluations

The clinical results are summarized in Table 3. Intraputaminal AAV-hAADC-2 infusion significantly improved both total and motor scores of the unified Parkinson's disease rating scale (UPDRS) in the OFF state. Five of six patients showed substantial improvement in UPDRS motor ratings in the OFF state (Figure 1). Changes in the UPDRS ON state and the percent of ON state hours in a day were not significant. One patient with relatively mild motor symptoms at baseline did not improve on UPDRS (A-3 in Figure 1). However, this patient showed a remarkable increase in mobile time as measured by the diaries (28% at baseline to 58% at 6 months after gene transfer; Figure 2). The daily dose of levodopa was unchanged in two patients (A-2 and A-5) and reduced in three patients (A-1, A-3, and A-5) at 6 months. Patient A-6, who had daytime sleepiness, preferred to reduce pramipexole instead of levodopa after gene therapy.

The last three patients underwent the levodopa test after our institutional review board confirmed the safety of AADC gene transfer in the first three patients. The short-duration response to levodopa did not change significantly after gene therapy in these three patients, though UPDRS motor scores at 6 months showed slight improvement at 30 minutes in patient 5 and at 120 minutes in patient 4 after levodopa intake (Figure 3). Significantly higher peak plasma levodopa concentrations were observed in these two patients after gene therapy.

The mini-mental state examination (MMSE) and geriatric depression scale (GDS) scores did not change significantly.

Table 3 Clinical outcomes of six patients

	Baseline	6 months	*P* value
UPDRS Total OFF	53 (12.4)	38 (10.1)	0.049*
UPDRS Total ON	15 (7.2)	10.7 (2.9)	0.262
UPDRS Part III (Motor) OFF	25.3 (9.4)	13.7 (6.0)	0.024*
UPDRS Part III (Motor) ON	5.2 (4.6)	1.8 (1.5)	0.120
Percent day spent in mobile state	48.8 (12.9)	55.4 (14.8)	0.348
Daily levodopa equivalents dose, mg	808 (169)	707 (233)	0.097

Abbreviations: OFF, off-medication state; ON, on-medication state; UPDRS, Unified Parkinson's Disease Rating Scale.
Data are presented as means (SD). The UPDRS scores in each patient did not change during the 2 months of the screening period.
*$P < 0.05$.

PET analysis

PET imaging revealed increased 6-[^{18}F]fluoro-L-*m*-tyrosine (FMT), a tracer for AADC, activity 4 weeks postoperatively, which persisted at 6-month evaluation (Figure 4). The mean increase in FMT uptake from baseline in the combined (right and left) putamen at 24 weeks was 56%. Two patients (A-1 and A-2) who had PET scans 96 weeks after surgery showed persistently increased FMT uptake. In these two patients, motor performance in the OFF state also maintained its improvement at 96 weeks.

DISCUSSION

Extensive preclinical studies on both rodent and nonhuman primate models of PD have shown that AAV vectors can express exogenous genes for a long time in the brain target areas without

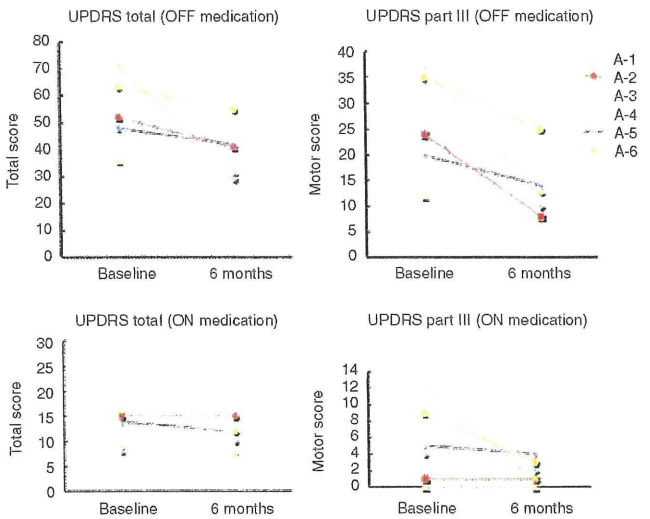

Figure 1 Changes in UPDRS scores. Absolute changes in scores from baseline to 6 months for individual patients. OFF, off-medication state; ON, on-medication state; UPDRS, Unified Parkinson's Disease Rating Scale.

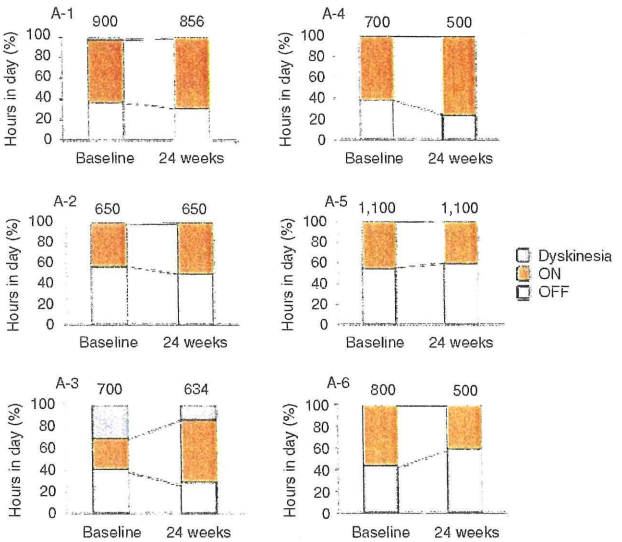

Figure 2 Evaluation of patients' diaries and daily doses of levodopa equivalents. For each 30-minute interval throughout the day, the patients recorded whether they were mobile (ON), immobile (OFF), or asleep. They also recorded the time with troublesome dyskinesias (Dyskinesia). The graph shows the percentage of hours in a day spent in each condition at baseline and at 6 months. The numbers on the bars indicate the mean daily doses of levodopa equivalents (mg). OFF, off-medication state; ON, on-medication state.

significant toxicity.[3,4,6,8,9] Recently, three phase I clinical trials of gene therapy for advanced PD demonstrated that AAV vector–mediated gene delivery into the subthalamic nucleus or putamen was safe and tolerable.[10–13] In this study, the safety of the AAV vectors for clinical use in the human brain was confirmed. Although one patient developed a venous hemorrhage in the subcortical white matter along the trajectory, it is well known that cerebral bleeding occasionally occurs in association with surgical procedures for deep brain stimulation in which electrodes are inserted into the basal ganglia through the frontal lobe white matter.[14,15] PET imaging in this patient showed that putaminal AADC expression was not affected by the subcortical venous hemorrhage and persisted up to 96 weeks. Thus, the venous hemorrhage was probably due to the surgical procedure and not gene transduction.

Although the present trial was a small, open-label study, and the nonblinded, uncontrolled analysis limits the interpretation, the initial efficacy outcomes are encouraging. Our patients showed improved motor performance in the OFF state. Levodopa has a relatively short plasma half-life (60–90 minutes), and antiparkinsonian effects observed after levodopa administration have generally been recognized as short- and long-duration responses. The short-duration response roughly parallels the plasma levodopa concentrations and is thought to be closely linked to dyskinesia, whereas the long-duration response builds up over weeks and improves trough (worst) motor performance in the OFF state.[7] Because the pattern of the short-duration response to levodopa did not change after gene therapy in our patients, the beneficial effect on the OFF state appears to be attributed to augmentation of the long-term response to levodopa.[16] In the preclinical studies with animal models of PD, AAV vectors mainly transduced medium spiny neurons that have dopamine receptors, and extracellular dopamine was increased in the striatum after administration of levodopa.[5,17] The mechanism underlying the long-duration response is not sufficiently understood, and future study is necessary to determine how nonphysiologic production of dopamine in the striatal neurons could enhance the response. It has been reported that the sustained long-duration response to levodopa is greater in patients treated with higher single doses of levodopa.[18] Thus, it is likely that increased dopamine in the putamen after gene transfer may enhance the stable long-duration response. Motor fluctuations in PD are associated with increased response to levodopa with a deeper trough in motor performance, rather than shortening of the response. Improving trough or OFF state motor function by augmenting the long-term response would likely reduce motor fluctuation.[16] Two of three patients in whom the short-duration response to levodopa was studied showed increased peak plasma levodopa concentrations after gene therapy. This finding may simply reflect variable absorbance of levodopa, and it remains to be elucidated whether changes in gastrointestinal absorption could be related to better motor performance in the OFF state.[19]

Activities and levels of AADC mRNA and protein are profoundly reduced in advanced PD,[2] but there are still several types of AADC-containing cells in the striatum, such as serotonin neurons, intrinsic dopamine neurons, AADC-containing "D" neurons, and glial cells.[20] These cells may act as a local source of dopamine. However, dopamine produced in nondopamine cells may not be taken up into dopamine cells and stored in synaptic vesicles, as dopamine transporter and vesicular monoamine transporter 2 are also reduced in advanced PD. The functional efficacy of dopamine produced from exogenous levodopa in these cells may be limited, at least in primates.[2,3] Striatal output neurons, main targets in AADC gene therapy, play a principal role in dopamine modulation of motor function in the basal ganglia. Dopamine synthesized in the striatal neurons themselves may more easily stimulate both synaptic and extrasynaptic receptors.

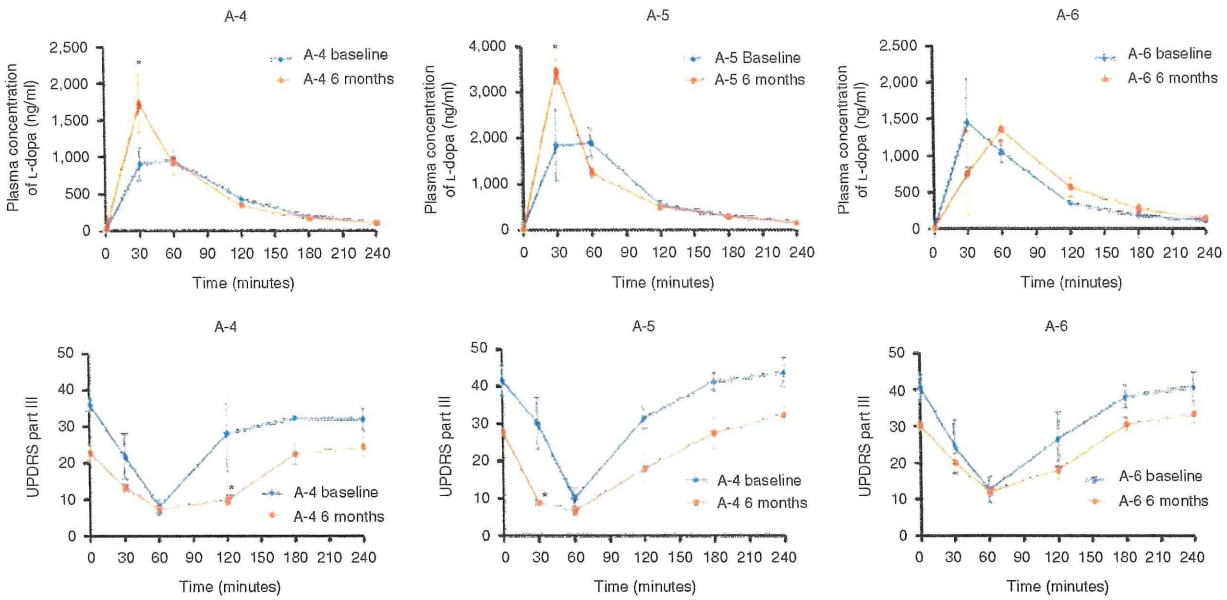

Figure 3 Short-duration response to levodopa. Comparison of short-duration response to levodopa before (blue) and after gene therapy (brown) in three patients (A-4, A-5, and A-6). Patients took 100 mg of levodopa with 25 mg benserazide orally after 20 hours without dopaminergic medication. Values represent means and SE of three trials. Upper panels: plasma levodopa levels; lower panels: Unified Parkinson's Disease Rating Scale motor scores. $^{*}P < 0.05$.

Results of a similar phase I protocol were reported recently for the 10 patients treated with AAV-hAADC-2 (ref. 10). That study used the same vector preparations as this study. The subjects were divided into two groups that received the same or one-third dose of the vector used in this study, respectively. Although the present patients had slightly milder initial symptoms, the patients treated with the same dose of vector in the two studies showed similar improvement in the OFF state and putaminal FMT uptake on PET. These findings provide independent confirmation of the safety, tolerability, and potential efficacy of AADC gene therapy. Future studies focusing on optimal vector dosing and defining the relationship between vector dose and clinical effects are necessary.[21]

In conclusion, these data indicate that AAV vector–mediated gene transfer of AADC is safe and may benefit advanced PD patients.

MATERIALS AND METHODS

Study design. The protocol and consent forms were approved by the institutional review board. The protocol was also reviewed by the committee of the Ministry of Health, Labour and Welfare of Japan. A data safety monitoring board reviewed the ongoing study. All subjects reviewed the consent form and provided their written, informed consent.

This 24-week, phase I, open-label study was primarily designed to evaluate the safety and tolerability of intraputaminal AAV-hAADC-2 infusion in idiopathic PD. Patients were evaluated preoperatively and monthly postoperatively for 6 months, using multiple measures, including the UPDRS, motor state diaries, the MMSE, the short form of the GDS, and laboratory tests. The UPDRS was done in the practically defined OFF state 12 hours after withdrawal of all antiparkinsonian medications, and in the ON state 1 hour after administration of the usual morning dose of medication. Motor scores for the UPDRS can range from 0 to 56, with higher scores indicating poorer function. Using diaries that separated the day into half-hour segments, the patients recorded their mobility during the 4 days before admission and for another 4 days at 6 months after admission. They were trained to rate their condition as sleeping, immobile, mobile without troublesome dyskinesias, or mobile with troublesome dyskinesias. The total number of hours spent in each of these categories was calculated, and the differences between the baseline and the 6-month scores were compared between the groups.

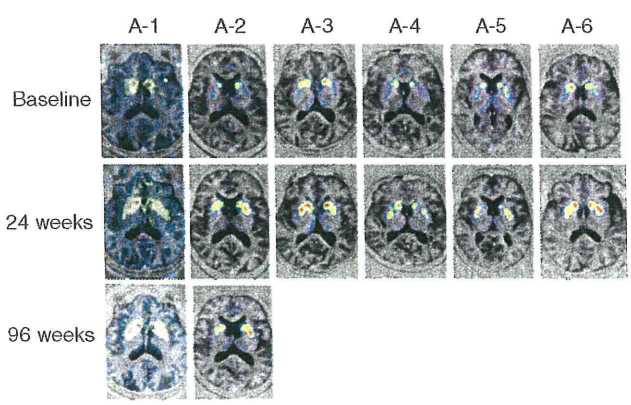

Figure 4 FMT-PET images. Axial images at the level of the putamen are shown before and 24 weeks after gene therapy for all six patients. Increased FMT uptake persisted until 96 weeks in two patients. The 4-week images are not shown because they are similar to the 24-week images. FMT, 6-[^{18}F]fluoro-L-*m*-tyrosine; PET, positron emission tomography.

The short-duration response to levodopa was evaluated in three patients (patients 4–6) at baseline and 6 months after gene transfer; they took 100 mg of levodopa orally with 25 mg benserazide after 20 hours without dopaminergic medication. Motor symptoms based on UPDRS motor (part III) and plasma levodopa concentrations were assessed at baseline and 30 minutes, 1, 2, 3, and 4 hours after levodopa intake.

Patients. The main entry criteria were: age 45–75 years; diagnosis of moderate to advanced PD, defined as Hoehn and Yahr Stage IV and UPDRS in the practically defined OFF condition of at least 20; at least

5 years of levodopa therapy; a minimum 8-point improvement in the UPDRS motor score after levodopa intake; and motor complications not satisfactorily controlled with medical therapy. The main exclusion criteria were atypical parkinsonism, dementia (MMSE score <20), and previous neurosurgical treatment for PD.

Vector and stereotaxic infusion. The vector used in this trial was a recombinant AAV2 with an expression cassette consisting of a human cytomegalovirus immediate-early promoter, followed by the human growth hormone first intron, complementary DNA of human AADC, and simian virus 40 polyadenylation signal sequence.[3–6] Clinical grade AAV-hAADC-2 was manufactured by Avigen (Alameda, CA) and provided by Genzyme (Boston, MA). The patients received AAV-hAADC-2 *via* bilateral intraputaminal infusions. Two target points were determined in the putamen that were sufficiently separated from each other in dorsolateral directions and identified on a magnetic resonance image. One burr hole was trepanned in each side of the cranial bone, through which the vector was injected into the two target points *via* the two-track insertion route. The vector-containing solution was prepared to a concentration of 1.5×10^{12} vector genome/ml, and 50 µl per point of the solution were injected at 1 µl/min; each patient received 3×10^{11} vector genome of AAV-hAADC-2.

Neutralizing antibody titers against AAV2 were determined by measuring β-galactosidase activities in HEK293 cells transduced with 5×10^3 vector genome/cell of AAV2 vectors expressing β-galactosidase in various dilutions of sera.[22]

PET. The AADC expression level in the putamen was assessed on PET imaging with FMT 6 days before surgery and 1 and 6 months after gene transfer. All patients stopped dopaminergic medications 18 hours before PET and took 2.5 mg/kg of carbidopa orally 1 hour before FMT injection. Subsequently, 0.12 mCi/kg of FMT in saline were infused into an antecubital vein, and a 90-minute dynamic acquisition sequence was obtained. The PET and magnetic resonance imaging data were co-registered with a fusion processing program (Syntegra; Philips, Amsterdam, The Netherlands) to produce the fusion images. Radioactivities within volumes of interest drawn in the putamen and occipital lobe were calculated between 80 and 90 minutes after tracer injection. A change in putaminal FMT uptake from baseline to 24 weeks was assessed using the putaminal–occipital ratio of radioactivities.

Statistical analysis. Values at baseline and 6 months after gene transfer were compared using Student's *t*-test (paired analyses). A two-sided *P* value <0.05 was taken to indicate significant differences. Two-way analysis of variance with Bonferroni correction of *P* values was used for the short-duration response to levodopa.

ACKNOWLEDGMENTS

This study was supported by grants from the Japanese Government: a grant-in-aid from the Research Committee of CNS Degenerative Diseases *via* the MHLW and grants from the Ministry of Education, Culture, Sports, Science and Technology. We thank Hiroshi Ichinose and Toshiharu Nagatsu for their helpful comments, and Naomi Takino, Hitomi Miyauchi, Keiko Ayabe, and Tetsuo Ito for their technical assistance. We also thank Avigen and Genzyme for providing clinical grade AAV vector.

REFERENCES

1. Fahn, S (2008). The history of dopamine and levodopa in the treatment of Parkinson's disease. *Mov Disord* **23** Suppl 3: S497–S508.
2. Nagatsu, T and Sawada, M (2007). Biochemistry of postmortem brains in Parkinson's disease: historical overview and future prospects. *J Neural Transm Suppl*: 113–120.
3. Bankiewicz, KS, Eberling, JL, Kohutnicka, M, Jagust, W, Pivirotto, P, Bringas, J *et al.* (2000). Convection-enhanced delivery of AAV vector in parkinsonian monkeys; *in vivo* detection of gene expression and restoration of dopaminergic function using pro-drug approach. *Exp Neurol* **164**: 2–14.
4. Bankiewicz, KS, Forsayeth, J, Eberling, JL, Sanchez-Pernaute, R, Pivirotto, P, Bringas, J *et al.* (2006). Long-term clinical improvement in MPTP-lesioned primates after gene therapy with AAV-hAADC. *Mol Ther* **14**: 564–570.
5. Muramatsu, S, Fujimoto, K, Ikeguchi, K, Shizuma, N, Kawasaki, K, Ono, F *et al.* (2002). Behavioral recovery in a primate model of Parkinson's disease by triple transduction of striatal cells with adeno-associated viral vectors expressing dopamine-synthesizing enzymes. *Hum Gene Ther* **13**: 345–354.
6. Shen, Y, Muramatsu, SI, Ikeguchi, K, Fujimoto, KI, Fan, DS, Ogawa, M *et al.* (2000). Triple transduction with adeno-associated virus vectors expressing tyrosine hydroxylase, aromatic-L-amino-acid decarboxylase, and GTP cyclohydrolase I for gene therapy of Parkinson's disease. *Hum Gene Ther* **11**: 1509–1519.
7. Nutt, JG (2008). Pharmacokinetics and pharmacodynamics of levodopa. *Mov Disord* **23** Suppl 3: S580–S584.
8. Leriche, L, Björklund, T, Breysse, N, Besret, L, Grégoire, MC, Carlsson, T *et al.* (2009). Positron emission tomography imaging demonstrates correlation between behavioral recovery and correction of dopamine neurotransmission after gene therapy. *J Neurosci* **29**: 1544–1553.
9. Muramatsu, S, Tsukada, H, Nakano, I and Ozawa, K (2005). Gene therapy for Parkinson's disease using recombinant adeno-associated viral vectors. *Expert Opin Biol Ther* **5**: 663–671.
10. Christine, CW, Starr, PA, Larson, PS, Eberling, JL, Jagust, WJ, Hawkins, RA *et al.* (2009). Safety and tolerability of putaminal AADC gene therapy for Parkinson disease. *Neurology* **73**: 1662–1669.
11. Eberling, JL, Jagust, WJ, Christine, CW, Starr, P, Larson, P, Bankiewicz, KS *et al.* (2008). Results from a phase I safety trial of hAADC gene therapy for Parkinson disease. *Neurology* **70**: 1980–1983.
12. Kaplitt, MG, Feigin, A, Tang, C, Fitzsimons, HL, Mattis, P, Lawlor, PA *et al.* (2007). Safety and tolerability of gene therapy with an adeno-associated virus (AAV) borne GAD gene for Parkinson's disease: an open label, phase I trial. *Lancet* **369**: 2097–2105.
13. Marks, WJ Jr, Ostrem, JL, Verhagen, L, Starr, PA, Larson, PS, Bakay, RA *et al.* (2008). Safety and tolerability of intraputaminal delivery of CERE-120 (adeno-associated virus serotype 2-neurturin) to patients with idiopathic Parkinson's disease: an open-label, phase I trial. *Lancet Neurol* **7**: 400–408.
14. Ben-Haim, S, Asaad, WF, Gale, JT and Eskandar, EN (2009). Risk factors for hemorrhage during microelectrode-guided deep brain stimulation and the introduction of an improved microelectrode design. *Neurosurgery* **64**: 754–62; discussion 762.
15. Weaver, FM, Follett, K, Stern, M, Hur, K, Harris, C, Marks, WJ Jr *et al.*; CSP 468 Study Group. (2009). Bilateral deep brain stimulation vs best medical therapy for patients with advanced Parkinson disease: a randomized controlled trial. *JAMA* **301**: 63–73.
16. Nutt, JG, Carter, JH, Lea, ES and Sexton, GJ (2002). Evolution of the response to levodopa during the first 4 years of therapy. *Ann Neurol* **51**: 686–693.
17. Sánchez-Pernaute, R, Harvey-White, J, Cunningham, J and Bankiewicz, KS (2001). Functional effect of adeno-associated virus mediated gene transfer of aromatic L-amino acid decarboxylase into the striatum of 6-OHDA-lesioned rats. *Mol Ther* **4**: 324–330.
18. Zappia, M, Oliveri, RL, Bosco, D, Nicoletti, G, Branca, D, Caracciolo, M *et al.* (2000). The long-duration response to L-dopa in the treatment of early PD. *Neurology* **54**: 1910–1915.
19. Cersosimo, MG and Benarroch, EE (2008). Neural control of the gastrointestinal tract: implications for Parkinson disease. *Mov Disord* **23**: 1065–1075.
20. Kitahama, K, Geffard, M, Araneda, S, Arai, R, Ogawa, K, Nagatsu, I *et al.* (2007). Localization of L-DOPA uptake and decarboxylating neuronal structures in the cat brain using dopamine immunohistochemistry. *Brain Res* **1167**: 56–70.
21. Forsayeth, JR, Eberling, JL, Sanftner, LM, Zhen, Z, Pivirotto, P, Bringas, J *et al.* (2006). A dose-ranging study of AAV-hAADC therapy in Parkinsonian monkeys. *Mol Ther* **14**: 571–577.
22. Ito, T, Yamamoto, S, Hayashi, T, Kodera, M, Mizukami, H, Ozawa, K *et al.* (2009). A convenient enzyme-linked immunosorbent assay for rapid screening of anti-adeno-associated virus neutralizing antibodies. *Ann Clin Biochem* **46**: 508–510.